Title
TOPOLOGICAL THEORY OF LEPTONS AND SCALAR BOSONS. II. DYNAMICS AND PHENOMENOLOGY

Author
Issler, D.

Publication Date
1985-11-01

Lawrence Berkeley Laboratory
UNIVERSITY OF CALIFORNIA

Physics Division

Submitted for publication

TOPOLOGICAL THEORY OF LEPTONS AND SCALAR BOSONS.
II. DYNAMICS AND PHENOMENOLOGY

D. Issler

November 1985

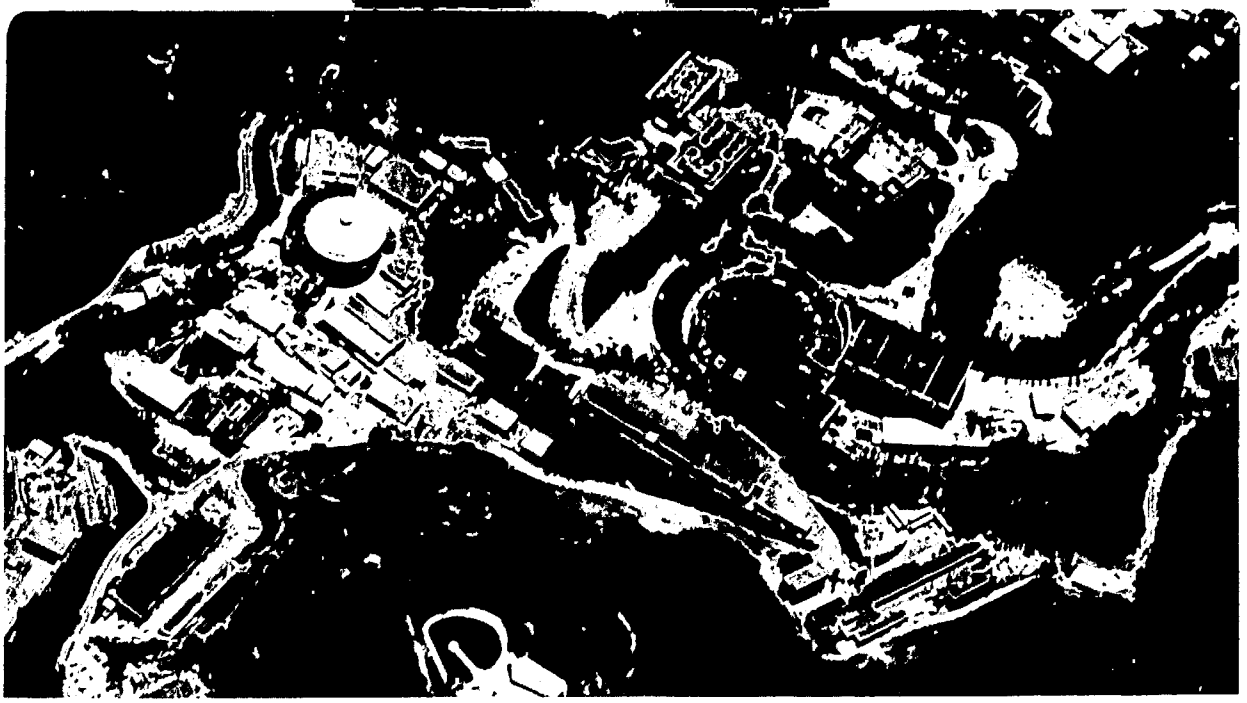

Prepared for the U.S. Department of Energy under Contract DE-AC03-76SF00098

DISCLAIMER

November 1985 LBL-20635

TOPOLOGICAL THEORY OF LEPTONS AND SCALAR BOSONS

(II) Dynamics and Phenomenology

Dieter Issler* †
Lawrence Berkeley Laboratory
and
Department of Physics
University of California
Berkeley, California 94720

ABSTRACT

The dynamical and phenomenological consequences of the topological model of nonhadrons and their interactions are investigated. The Feynman rules developed in the preceding paper correspond to those of a nonrenormalizable Lagrangian. Two different ways of precluding infinities and softening electroweak vertex functions at the TeV scale by means of strong interactions are discussed, both of which imply that the elementary electroweak vertex functions are determined by the strong interactions. Heavy hadrons also give large masses to seven of eight electroweak vector bosons and to all "horizontal" scalar bosons. Invoking a proposal of the preceding paper for generation-symmetry breaking couplings of heavy hadrons to the charged τ and λ leptons, the masses of e and μ are understood as radiative effects and imply $m_\lambda \sim 400\,\mathrm{GeV}$. Mixing between W_L and W_R leads to a similar mass hierarchy among neutrinos. The expected $L-R$ mixing angle is not in conflict with present mass limits for ν_e but violates the bound imposed on ν_λ by the standard cosmological model through the ^{4}He abundance. Strict conservation of lepton-generation numbers is supported by the data.

*Address after January 1, 1986: Institut f. Theor. Physik, Universität Bern, Sidlerstrasse 5, CH-3012 Bern, Switzerland

†This work was supported by the Director, Office of Energy Research, Office of High Energy and Nuclear Physics, Division of High Energy Physics of the US Department of Energy under contract DE-AC03-76SF00098

1 Introduction

This is the second of a series of two papers which investigate ways of describing the properties and interactions of leptons in the framework of topological particle theory (TPT) [1,2,3] which began as a theory of the strong interactions. TPT is not a quantum field theory but is based on S-matrix principles which are implemented through a graphical expansion; the latter is ordered by the topological complexity of bounded two-dimensional surfaces embedding the Feynman graph [4,5,1]. These surfaces are patched by several types of lines which also cut the surface boundary into segments. Particles are represented by combinations of such segments and inherit their discrete quantum numbers from the orientations of lines ending on them and of adjacent patches as well as their boundaries. The known physical hadrons are reproduced and a huge class of very heavy exotic mesons ("hexons") [6] is predicted which will play a significant role in the present context.

As in QCD, TPT hadrons are extended objects, but they do not consist of point-like elementary quarks and gluons; instead, any elementary state in TPT is a bound state of all other elementary states. The lowest level in the topological expansion produces a closed (infinite) system of coupled nonlinear equations through which the elementary vertex functions determine themselves (bootstrap) [3,7,8]. Feynman-like rules were established, from which higher orders can in principle be calculated [9].

The preceding paper ([10], hereafter referred to as [I]) adapted earlier proposals for the incorporation of nonhadrons to recent changes in TPT [2]. Electroweak particles are constructed in close analogy with hadrons, but they also have to be distinguishable from the latter. That requirement admits just eight chiral vector bosons associated with the group $U(2)_R \times U(2)_L$, four generations of isodoublet Dirac leptons and eight neutral scalar bosons $H_{GG'}$. The latter couple to the generation

degree of freedom on leptons; only the combinations $GG' = e\mu,\ e\tau,\ \mu\lambda,\ \tau\lambda$ occur (λ designates the predicted fourth lepton generation).

Detailed proposals were made in [I] for the structure of surfaces embedding elementary nonhadron vertices, from which Feynman rules could be deduced. They are the same as those obtained – at the tree level and in Landau gauge – from the Lagrangian

$$\begin{aligned}\mathcal{L} \;=\; & -\tfrac{1}{8}\,\mathrm{Tr}\,(F^R_{\mu\nu}F^{\mu\nu}_R + F^L_{\mu\nu}F^{\mu\nu}_L) \\ & +\sum_G\ \overline{\psi}_G(i\gamma\cdot\partial - g\,V_R\cdot\gamma\tfrac{1+\gamma_5}{2} - g\,V_L\cdot\gamma\tfrac{1-\gamma_5}{2})\,\psi_G \\ & +\sum_{G,G'}\ \Big\{\tfrac{1}{2}\,\mathrm{Tr}\,[\,\tfrac{1}{2}(\partial_\mu H_{GG'})(\partial^\mu H_{G'G}) \\ & \qquad +ig(\partial_\mu H_{GG'})H_{G'G}\tfrac{1-\gamma_5}{2}(V_R^\mu + V_L^\mu) \\ & \qquad -g^2 H_{GG'}H_{G'G}\tfrac{1-\gamma_5}{2}V_\mu^R\tfrac{1-\gamma_5}{2}V_L^\mu\,\Big] \\ & \quad -f H_{GG'}\,\overline{\psi}_{G'}\,\psi_G\ \Big\}.\end{aligned} \tag{1}$$

V_L and V_R are 2×2 matrix fields in isospin space, in which $\vec{\tau}$ designates the Pauli matrices. ψ_G and $\overline{\psi}_G$ are isospinor Dirac four-spinors with generation label G. The field strengths are given by

$$F^{R(L)}_{\mu\nu} := \partial_{[\mu}V^{R(L)}_{\nu]} + igV^{R(L)}_{[\mu}V^{R(L)}_{\nu]}.$$

H bosons obey the relation $(H_{G'G})^\dagger = H_{GG'}$.

The last few terms in (1) are not invariant under chiral transformations and under isospin rotations. Accordingly, certain infinities arising in loop diagrams cannot be absorbed in the renormalization of wave functions and coupling constants. A particular example are the two-loop graphs in Fig.1 which produce mixing between V_L and V_R. (The notation is as in Fig.20 of [I]: wiggly lines for vector bosons, dashed lines for H bosons and full lines for leptons, with arrows indicating the flow of lepton-generation numbers.)

The following section will discuss various approaches to a future solution of the problem. No satisfactory way of making TPT either renormalizable or finite without recurrence to hadrons is found. It is then asked whether a nonperturbative treatment of radiative corrections from hadrons might "soften" electroweak vertices and make radiative corrections from nonhadrons finite. The topological expansion may be defined in such a way that calculation of nonhadron loops is postponed until an infinite class of hadronic radiative corrections has been incorporated in electroweak vertices and propagators through an intermediate renormalization. The high masses $m_0 \geq 1$ TeV and huge multiplicity of elementary hadrons make the nonhadrons appear as bound states of hadrons and nonhadrons with radii $\sim m_0^{-1}$, without changing their low-energy characteristics very much. A study of the discontinuity structure of renormalized vertex functions indicates, however, that electroweak loop diagrams may continue to diverge if elementary nonhadrons are hard, point-like objects.

If this preliminary conclusion is confirmed, TPT nonhadrons require a substructure that must have certain features in common with the fundamental strong-interaction bootstrap dynamics reviewed in Appendix A. One approach, identifying that substructure with the TeV-scale strong interactions themselves, is sketched in Appendix B; it may be able to determine the fine-structure constant dynamically.

For the purpose of the brief phenomenological analysis of the model, presented in Sect.4, the Lagrangian (1) is used as effective low-energy approximation and supplemented by hadronically generated mass terms for all vector bosons (except the photon), all H bosons and the λ and τ leptons. Higher-order electroweak effects are responsible for the masses of e, μ and all neutrinos (the latter are Dirac fermions and stable in TPT). Mass estimates presented in Sect.3 reproduce the data well with reasonable choices for those parameters which have not been calculated yet (coupling constants). The old idea that the ratio m_e/m_μ might be connected to the

fine-structure constant is revived by TPT in a somewhat modified form. (A short account of these results was given in a recent Letter with Chew [11].)

Although the underlying topological structures strongly constrain this model, there is no apparent conflict with present experimental data, but effective methods for calculating and summing large classes of strong-interaction diagrams are needed before definite conclusions regarding, *e.g.*, neutrino masses can be drawn. Section 4 shows that the stringent lower bounds on the mass scale of new weak interactions connected with fermion generations (see [12], *e.g.*) do not apply to TPT because of strict conservation of lepton-generation numbers. Conversely, the experimental observation of certain forbidden decays like $p \to X$ and $\mu \to 3e$ would immediately disprove the model proposed here. The major phenomenological problem is the bound on neutrino masses indirectly obtained from the observed ^{4}He abundance and the standard cosmological model.

2 Renormalization

2.1 The Need for Finite Renormalizations in TPT

With respect to renormalization, TPT occupies an intermediate position between local quantum field theory, where physical states are superpositions of infinitely many elementary-particle states and the fundamental parameters of the theory undergo renormalization, and S-matrix bootstrap approaches, which deal with physical quantities and states only: Renormalization is necessary in TPT because the topological expansion distinguishes between elementary and physical particles. On the other hand, elementary hadrons emerge from the bootstrap dynamics at the basis level of the topological expansion as bound states of indefinite numbers of their own kind – there are no structureless elementary hadron states in TPT. The concomitant self-determination of zero-entropy vertex functions ([6,7,8], see also Appendix A) is meaningful only if all parameters are finite – the zero-entropy bootstrap is in this respect similar to the full bootstrap at the level of the physical S matrix. The nonlinearity of the bootstrap system precludes absorption of infinities potentially arising in radiative corrections through infinite renormalization of bare parameters. Appendix A argues that the strong-interaction topological expansion is indeed finite term by term due to the special properties of zero-entropy vertex functions.

TPT's electroweak sector so far has been developed in fairly close analogy to renormalizable gauge theories. If elementary nonhadrons are viewed as structureless and hadrons were decoupled from the electroweak sector, the single terms in the perturbative expansion would generally be infinite. As seen in Sect.1, certain divergences could not be renormalized away and would make the theory inconsistent. One may hope to resolve the dilemma in one of the following ways (or maybe

by a combination thereof):

1. Change the nonhadron spectrum and interactions in such a way that the theory becomes renormalizable or finite, or

2. Soften structureless elementary vertices by including an infinite sum of radiative corrections from hadrons, or

3. Discard the notion of structureless elementary particles and vertices by introducing a compositeness scale for nonhadrons.

Following the first option, one may turn (1) into a renormalizable Lagrangian by removing H's altogether or by eliminating all axial-vector components of the gauge fields together with the $H - V^{n\bar{n}}$ couplings, or by making H bosons transform as **(2,2)** under $U(2)_R \times U(2)_L$. Neither avenue appears consistent with the underlying topological structures [I]. Even if it could be done, this approach would be unsatisfactory in that it forestalls direct determination of electroweak (bare) coupling constants from the strong interactions, since these quantities cannot be finite if divergences occur in loop diagrams. Similarly, no standard supersymmetry algebra has been found compatible with the model. (Various conflicts between the Majorana character of SUSY generators and TPT's chiral structure arise; also, internal degrees of freedom assume different roles on bosonic and fermionic constituents.)

The second and third approaches agree in their emphasis on additional, more fundamental interactions producing effects that are not describable in any finite order of perturbation theory. Either the effective or the fundamental electroweak vertices are supposed to possess enough structure to decrease at high q^2 and thereby to prevent divergences in loop diagrams. This can happen, however, only if the fundamental dynamical mechanism producing the softening operates at a level of

the topological expansion *below* the appearance of the first nonhadron loop. One is thus led to consider the proper definition of the topological expansion of amplitudes containing nonhadrons.

2.2 The Topological Expansion of Electroweak Amplitudes. Skeleton Graphs

The distinction, in the topological expansion of strong-interaction amplitudes, of first-kind and second-kind entropy indices, has proved useful. The former (g_1 and g_2, genus and number of boundary components) have direct counterparts in 't Hooft's $1/N$ expansion of gauge theory [13]. The recognition of second-kind entropy (g_3 and g_4, connected to chiral and colour switching) [14] was instrumental in the reduction of the zero-entropy bootstrap problem to its simplest form and in the extension of TPT to the electroweak interactions. Second-kind entropy does not necessarily suppress amplitudes, but may even substantially enhance them; at the same time it reduces the number of poles in the S matrix. It has often been found useful [9,6] to consider classes of diagrams with prescribed first-kind entropy and indefinite second-kind entropy (see **(29)** as a case in point). It is quite possible that different orders of summing over entropy indices give different physical amplitudes; the irrelevance of second-kind entropy to field theory and the comparable magnitude of terms with grossly different g_3 or g_4 suggest a hierarchy of entropy indices where, for each fixed value of g_1 and g_2, summation over all values of g_3 and g_4 is carried out. Its usefulness in the electroweak case (see below) strengthens this conjecture.

Given the fundamental differences between elementary hadrons and nonhadrons, are there additional entropy indices to characterize the electroweak nature of a graph? In view of ultraviolet divergences it is meaningful to define a ("strong")

entropy index g_5 as the number of nonhadron loops in a graph. If g_5 is attributed the same (or higher) rank in the entropy hierarchy as g_1 and g_2, infinite numbers of hadronic radiative corrections to electroweak vertices have to be summed and included even in the simplest nonhadron loop diagram. The effects of such partial renormalization by hadrons will be discussed in the next subsection.

A characteristic feature of nonhadrons is the occurrence of kinetic-energy trivial vertices in propagator lines (see [I], Sect.4.2). g_5 may thus be defined in a more topological way as the number of Feynman loops along which kinetic-energy vertices alternate with nontrivial vertices[1]. All hadronic (strong-interaction) graphs have $g_5 = 0$, as do electroweak tree graphs with any number of hadronic radiative corrections.

The above definition of g_5 has a shortcoming connected with hadron–vector-boson vertices. Figure 2(b), while obviously a hadronic radiative correction to Fig.2(a), would have to be attributed lower g_5 because the nonhadron loop is interrupted by the hadronic self-energy insertion. The definition of g_5 may be amended so that both graphs have $g_5 = 1$, but the immediate topological meaning of this index is then obscured. Assuming that future investigations will clarify this point, the latter, more physical interpretation of g_5 will be adopted in the following. (Note that this ambiguity does not arise for leptons and H's because lepton-generation number is absolutely conserved and is not carried by hadrons.)

It is useful now to introduce skeleton graphs [15] which incorporate, in a single diagram, an infinite sum of graphs and whose vertices and lines correspond to (hadronically) renormalized interactions and particles. The skeleton S of a Feynman graph F is obtained by shrinking all its connected purely hadronic subgraphs to

[1]Nonhadron kinetic-energy trivial vertices are clearly distinguishable from zero-entropy trivial vertices (see Appendix A and [9]) by their intrinsic complexity.

little blobs. Vector-boson lines always attach to the boundary of such bubbles; they may begin and end on the same partially renormalized vertex (producing thereby a graph with $g_5 > 0$). Lepton and H-boson lines cross the bubbles, and the $H\bar{l}l$ vertex is "buried in the hadron cloud"[2]. Figure 3 gives a typical example of a skeleton graph: Every vertex and every propagator contain an infinite number of radiative corrections; effective vertices with any number of lines may appear. The situation is quite analogous to that of an effective Lagrangian theory after heavy degrees of freedom have been integrated out of the fundamental action.

2.3 Properties of Partially Renormalized Vertex Functions

The properties of the above-defined effective vertices are crucial for both theoretical and phenomenological analyses of the present model. A precise determination of these vertex functions is far beyond the scope of the present work: Neither is the precise structure of elementary semihadronic couplings known, nor do adequate nonperturbative methods exist for evaluating the infinite series of graphs involved. Some general properties may nevertheless be inferred by studying the discontinuity structure of partially renormalized vertices (PRV) and comparing them to zero-entropy vertices.

Figure 4 exhibits the discontinuities contained in a (partially renormalized) vector-boson self-energy and a cubic Yang–Mills vertex. On the right-hand sides, the first terms in the series represent the zero-mass elementary vector-boson pole and the elementary Yang–Mills coupling, respectively. The terms of (a) enclosed in brackets do not conserve the isospin currents [16] (the electric current is conserved,

[2]Conservation of lepton-generation number implies that an effective vertex with an odd number of H bosons must contain at least one elementary $H\bar{l}l$ vertex since hadrons do not carry lepton number.

however) and are expected to give masses to seven of the eight gauge bosons. In (b) the first term is put in brackets because it does not have a discontinuity if it is structureless as in QFT (for further discussion of this point see below).

Figure 4 clearly shows three important properties of this dynamics: Firstly, the hadronic effects are at low energies suppressed roughly as q^2/m_0^2 but, secondly, the contributing intermediate states have high multiplicity $\sim N^n$ where $N \sim 10^2$ is the effective diquark multiplicity (4^2 generations, 2^2 isospins, 2^2 spins, reduced by a factor 2 because of colour-space projections) and n counts intermediate hadron lines. One may thus expect that each term contributes above its threshold about as strongly to the total discontinuity as does each of its predecessors at the same q^2. Finally, the softness of hadronic vertex functions ensures the validity of unsubtracted dispersion relations for all terms *with intermediate hadrons* (see Appendix A).

A similar situation is encountered with leptons and H bosons, as illustrated by Fig.5. H bosons may be expected to become massive in the process while lepton mass terms are possible only where chiral symmetry is broken, *i.e.*, for τ and λ (see Sect.3 for details). One concludes again that the hadronic contribution to self-energies and vertex corrections satisfies unsubtracted dispersion relations and exhibits softness similar to that of purely hadronic vertex functions.

The condition for the second option listed in Sect.2.1 to be viable, *i.e.*, to make electroweak loops ($g_5 > 0$) finite, is that all PRV's vanish sufficiently rapidly as $p^2 \to \infty$ in any leg. It appears then natural to suppose that they satisfy unsubtracted dispersion relations in all their variables. On the other hand, a glance at Figs.4 and 5 shows that at least certain PRV's contain an elementary electroweak vertex, which by assumption does not have a discontinuity. The only possibility for reconciling these two conflicting statements comes from the *infinite sum* of discontinuities with intermediate hadrons: While each term separately tends to zero for large p^2, the

sum may be a (generally infinite) constant. If this is the case, one can identify the subtracted piece with the hard elementary vertex, going back to the posture of QFT, according to which bare coupling constants are meaningless and not finite. What has potentially been gained in the process (if it works consistently) is a way of dynamically determining the nonhadronic PRV's: The elementary hard vertices serve merely to cancel the divergences arising in the summation over infinitely many semihadronic Feynman graphs, and it is the latter which produce the renormalized nonhadronic vertex functions.

It is not presently possible to determine the asymptotic behaviour of the summed hadronic terms. If the asymptotic cancellation of semihadronic and hadronic vertex functions does not take place, the assumption has to be given up that elementary nonhadron vertices are structureless as in QFT; a true bootstrap dynamics will take the place of the bare Lagrangian (1), which may still be valid as a low-energy approximation to the full theory. Appendix B suggests that such a dynamics could indeed be developed.

In order to proceed despite the present uncertainty in this question it will be assumed in the remainder of this paper that (1) indeed describes the low-energy sector correctly when mass terms generated by hadrons (see Sect.3) are taken into account at zeroth order. Radiative corrections from nonhadrons will be estimated by calculating either the relevant Feynman diagram with a cut-off $\Lambda \approx 2m_0 \geq 2\text{TeV}$ or the corresponding dispersion integral with the discontinuity set to zero above $x_0 \approx 4m_0^2$. Radiative corrections from nonplanar hadron bubbles will be suppressed in the sense of the $1/N$ expansion, with $N \sim 10^2$ again being the effective diquark multiplicity, and can be safely neglected in most cases of practical interest.

3 The Mass Spectrum

TPT does not contain elementary Higgs bosons (H's carry non-zero conserved quantum numbers) and instead generates all nonhadron masses dynamically by means of electroweak interactions with hadrons. At this stage, only qualitative inferences on the size of these masses can be made from dimensional arguments and from counts of the number of hadronic states contributing to the nonhadron self-energies. An exception are interesting mass relations among leptons which result from an essentially perturbative mechanism responsible for the masses of e, μ and the neutrinos. The questions connected with gauge degrees of freedom of vector bosons will not be addressed here.

3.1 Electroweak Boson Masses

Hadronic self-energy insertions of the kind shown in Fig.6 produce mass for electroweak bosons if in (a)

$$N_H \Pi_H(q^2 = 0) \neq 0$$

and in (b)

$$N_V \Pi_V^{\mu\nu}(q^2) \not\to N_V(-q^2 g^{\mu\nu} + q^\mu q^\nu)\pi_V(q^2)$$

as $q^2 \to 0$.[3] Π_H and Π_V are defined as the self-energies produced by hadrons, with the quark or diquark state on the periphery of the bubble[4] held fixed. N_H and N_V are the numbers of different peripheral quark and diquark states which communicate with a given H-boson or vector boson state. No symmetry requires

[3] The self-energy insertions are not expected to exhibit a massless pole and thereby to break gauge symmetries spontaneously.

[4] In leading diagrams, the external nonhadrons must all couple to the same quark or diquark line which is therefore called peripheral.

Π_H to vanish at $q^2 = 0$; one expects $\Pi_H(0) \sim m_0^2$ on dimensional grounds. The resulting H-boson mass is

$$m_H^2 \approx F N_H \Pi_H(0) \tag{2}$$

where F is the (presumably rather small) coupling constant of an H pair to a hadronic bubble with specified peripheral quark or diquark. From the topological structures proposed in [I] it is inferred that $N_H \sim 2^5$ (4 quark generations, 2^2 isospins and 2 spins are free on a diquark coupled to H's). In view of these considerations it will henceforth be assumed that

$$m_H^2 \lesssim m_0^2. \tag{3}$$

The upper bound on m_H follows from the fact that H may also be viewed as a bound state of itself and a hexon, which is stable against hexon emission only if $m_H < m_0$.

For vector bosons, matters are complicated by the poor knowledge about the structure of the relevant semihadronic vertices, and uncertainty persists on the amount of symmetry breaking and current non-conservation. The electromagnetic current being absolutely conserved, the photon is expected to stay massless. In all other cases, the vacuum-polarization tensor may contain an extra piece $\pi_S(q^2)$:

$$\Pi_V^{\mu\nu}(q^2) = (-q^2 g^{\mu\nu} + q^\mu q^\nu)\,\pi_V(q^2) + g^{\mu\nu} m_0^2\,\pi_S(q^2), \tag{4a}$$

$$\pi_S(q^2 = 0) \neq 0. \tag{4b}$$

No attempt will be made here to find approximate expressions for the divergence of the isospin currents induced by the vector-boson–hadron couplings and to relate them to $\pi_S(q^2)$. At this point the assumption $\pi_S(0) \lesssim 1$ appears plausible and is in line with (3). The vector-boson masses are then given by

$$m_V^2 \approx e^2 N_V m_0^2\,\pi_S(0) \lesssim e^2 N_V m_0^2 \tag{5}$$

where $N_V \leq 2^6$, leading to masses near m_0. It has been suggested that N_V might be considerably smaller for left-handed vector bosons (except the left-handed part of the photon) on topological grounds [17], maybe explaining their intermediate masses.

Ref.[16] showed how mechanisms similar to those at work in meson physics may produce the electroweak-boson spectrum of the GSW model for γ, Z^0, $W_L^{\pm}$ while assigning significantly higher masses to $W_R^{\pm}$, $Z^{0\prime}$ and $Z^{0\prime\prime}$.

3.2 Lepton Masses Generated by Hadrons

TPT strictly conserves lepton-generation numbers and hence does not allow Majorana mass terms for leptons. Another unusual feature of the theory is that chiral symmetry cannot be broken spontaneously because the Feynman graphs are not just an approximation to an underlying field theory with a possibly asymmetric vacuum: If elementary TPT-lepton propagators maintain chiral symmetry, elementary TPT leptons have zero bare mass; if no elementary vertex broke chiral symmetry, even physical leptons would be massless. This means that at the electroweak tree level ($g_5 = 0$) only λ and τ may be massive because they have scalar couplings to hadrons (see Appendix A of [I]).

In Fig.7 a representative example is shown for each of the two lepton-hadron couplings that violate chiral symmetry: In (a) the λ lepton couples to a pair of elementary hexons (or maybe also baryons) which join to form a loop. The vacuon Θ, an anomalous neutral scalar particle [18,3] may in addition also couple to τ. It has not been determined whether graphs with a single vacuon coupling to a hadronic bubble are admissible in the topological expansion; they would correspond to a vacuum expectation value of Θ in a field theory and do not possess discontinuities.

Following the reasoning in the previous subsection one expects the graphs of the type shown in Fig.7(a) to contribute to m_λ with $m_4' \lesssim m_0$. The lower mass and weaker interactions of Θ introduce a smaller scale into the dynamics of Fig.7(b). It is therefore likely that Θ's contribution m_3 to m_λ ($m_\lambda \approx m_4 \equiv m_4' + m_3$) and m_τ is suppressed by some power of the ratio m_Θ/m_0. m_Θ can in principle be calculated from the cylindrical bootstrap system, once the planar system has been solved [3]. When the known lepton masses are extrapolated to m_λ in Sect.3.3, it is seen that a ratio $m_3/m_4 \approx 10^{-2}$ is required for fitting the data.

3.3 Lepton Masses from Electroweak Interactions

This subsection essentially reproduces the mass estimates presented in [11]. At the level of electroweak radiative corrections ($g_5 > 0$), the chiral-symmetry-breaking $H\bar{l}l$ couplings are able to produce mass terms if one already massive lepton is involved. Figure 8 shows the leading diagrams in the charged-lepton self-energies. λ gives rise to the μ mass and adds to the τ mass; both μ and τ have negligible effect on m_λ. m_μ and m_τ are the starting point for the electron mass which in turn has a very small impact on m_μ and m_τ. The absence of $H_{\lambda e}$ from the H-boson spectrum is at the root of this mass hierarchy.

The diagrams in Fig.8 would be logarithmically divergent in field theory; the infinity would have to be absorbed in (infinite) multiplicative renormalization of the bare mass which therefore is devoid of physical significance. The vertex softening discussed in the previous section makes the above self-masses finite and preserves the meaning of zero bare masses. A first estimate of m_μ and m_e is obtained by applying Feynman rules and cutting the loop momenta off at a value $\Lambda \sim m_0 \geq 1$

TeV:

$$m_2 = \Delta m_3 \approx m_4 \cdot \frac{\alpha_f}{4\pi} \cdot \left[\frac{m_H^2 + m_4^2}{m_0^2} + \left(1 - \frac{m_4^2}{m_H^2}\right) \ln\frac{m_0^2}{m_H^2} - \frac{m_4^2}{m_H^2} \ln\frac{m_H^2}{m_4^2}\right], \tag{6a}$$

$$m_1 \approx (m_2 + m_3 + \Delta m_3) \cdot \frac{\alpha_f}{4\pi} \cdot \left[\frac{m_H^2}{m_0^2} + \ln\frac{m_0^2}{m_H^2}\right]. \tag{6b}$$

where $\alpha_f \equiv f^2/4\pi$ and f is the Yukawa-type H–lepton coupling constant. m_2 and Δm_3 are found to depend somewhat (within a factor 2) on the ratios of m_4, m_H and m_0. Because $m_{2,3} \ll m_H$, only the ratio m_H/m_0 affects m_1.

m_4 may be identified with m_λ to very good approximation. While all relevant hadronic corrections to m_λ are already incorporated in m_4, one may not *a priori* identify m_1, m_2 and m_3 with m_e, m_μ and m_τ, respectively, because diagrams like that of Fig.9 may be significant. They are suppressed by the masses of the hadrons forming the bubble, but there is also a superficially quadratic divergence, cut off around m_0^2, from the loop integration. The smallness of the coupling may be balanced by the high multiplicity of the peripheral quarks and diquarks, thus no definite conclusion can presently be drawn.

An estimate of m_λ, free of this ambiguity, may be obtained from (6a), (6b) if the known masses of e, μ and τ are used as input. Summarizing the effect of hadronic corrections on m_e and m_μ in factors R_e and R_μ, one expects $R_e \approx R_\mu$. Accordingly, the relations

$$\begin{aligned} m_e &= R_e\, m_1 \approx R_e\, q_1 (m_\tau + m_\mu), \\ m_\mu &= R_\mu\, m_2 \approx R_\mu\, q_2 m_\lambda \end{aligned} \tag{7}$$

with

$$\begin{aligned} q_1 &\approx \frac{\alpha_f}{4\pi} \cdot \left[\frac{m_H^2}{m_0^2} + \ln\frac{m_0^2}{m_H^2}\right], \\ q_2 &\approx \frac{\alpha_f}{4\pi} \cdot \left[\frac{m_H^2 + m_\lambda^2}{m_0^2} + \left(1 - \frac{m_\lambda^2}{m_H^2}\right) \ln\frac{m_0^2}{m_H^2} - \frac{m_\lambda^2}{m_H^2} \ln\frac{m_H^2}{m_\lambda^2}\right] \end{aligned} \tag{8}$$

may be used to express m_λ implicitly through the equation

$$m_\lambda \approx \frac{m_\mu(m_\tau + m_\mu)}{m_e} \cdot \frac{q_1}{q_2} \equiv M \cdot \frac{q_1}{q_2}. \tag{9}$$

One may consider some special cases of (9):

$$m_\lambda \ll m_H: \quad m_\lambda \approx \frac{m_\mu(m_\tau + m_\mu)}{m_e} \approx 0.4\,\text{TeV}, \tag{10a}$$

$$m_\lambda = m_H \approx m_0: \quad m_\lambda \approx M \cdot \frac{1}{2} \approx 0.2\,\text{TeV}, \tag{10b}$$

$$m_\lambda = m_H \ll m_0: \quad m_\lambda \approx M \cdot \frac{m_0^2}{2m_\lambda^2} \cdot \ln\frac{m_0^2}{m_\lambda^2} \gg m_0, \tag{10c}$$

$$m_H \ll m_\lambda \approx m_0: \quad m_\lambda \approx M \cdot \frac{\ln(m_\lambda^2/m_H^2)}{1 + \ln(m_\lambda^2/m_H^2)} \lesssim 0.4\,\text{TeV}. \tag{10d}$$

Among them, only (a) provides a satisfactory solution, allowing both m_H and m_0 to be in the vicinity of 1 TeV. In what follows, this mass value will be adopted as TPT's prediction.

An estimate of α_f depends directly on the unknown ratio R_e; assuming $m_H \leq m_0 \leq 10 m_H$, one obtains

$$3.4 \cdot 10^{-3} \geq R_e \alpha_f \geq 7.4 \cdot 10^{-4}, \tag{11}$$

a value not too different from the gauge coupling.

It follows from the foregoing that the vacuon–τ coupling must give the latter a mass

$$m_3 \approx m_\tau - R_\mu m_2 \approx m_\tau - m_\mu \approx 1.7\,\text{GeV} \tag{12}$$

if the model is to meet experiment. m_3 thus has to be smaller than m_4 by about two orders of magnitude, a value which may appear not implausible in the light of the discussion given in Sect.3.2. Thus most of m_τ derives from the vacuon. H bosons put μ and τ on the same level in the mass hierarchy. Because of the conservation of lepton generations, the two states cannot repel through mixing – the explanation of

the $\mu - \tau$ mass difference must necessarily involve extra couplings of τ, not available to μ and not connected to electroweak bosons.

No analogous mass-generating mechanism can work for neutrinos unless at least one of them has acquired mass from some other source. The only way in which that can happen is interaction with a state containing a massive charged lepton. Both hadrons and H's couple only to neutral currents while elementary W's have chirally symmetric lepton couplings. At higher orders of the electroweak interactions (see Fig.1) or in the process of partial renormalization by hadrons some $W_L - W_R$ mixing will occur (this point will be discussed further in Sect.4):

$$\begin{aligned} W_L' &= W_L \cos\theta_\chi - W_R \sin\theta_\chi, \\ W_R' &= W_L \sin\theta_\chi + W_R \cos\theta_\chi \end{aligned} \tag{13}$$

are the rotated states with masses M_L and M_R, respectively. The two terms in Fig..5 are then easily evaluated and give[5]

$$\Delta m_\nu \approx m_l \cdot \frac{\alpha}{2} \cdot \frac{3}{4\pi} \cdot \sin\theta_\chi \cdot \ln(M_R^2/M_L^2) \tag{14}$$

where $\cos\theta_\chi \approx 1$ and $g_L g_R \approx e^2/2$ were used.

Chiral symmetry being broken, H bosons contribute to the neutrino masses in the same way as for charged leptons. In terms of q_1 (see (8)) and the quantity

$$r \equiv \frac{3\alpha}{8\pi} \cdot \sin\theta_\chi \cdot \ln(M_R^2/M_L^2) \tag{15}$$

[5] Following the Feynman rules given in [I], Sect.6, the Landau gauge was chosen. If the unitary gauge is to be used after the gauge bosons have acquired mass, the logarithmic factor in (14) changes to $(m_0/M_L)^2$.

the neutrino masses are given by

$$\begin{aligned} m_{\nu_\lambda} &\approx r \cdot m_\lambda, \\ m_{\nu_\tau} &\approx r \cdot m_\tau + q_1 \cdot m_{\nu_\lambda} \approx r \cdot m_\tau, \\ m_{\nu_\mu} &\approx r \cdot m_\mu + q_1 \cdot m_{\nu_\lambda} \approx 2r \cdot m_\mu, \\ m_{\nu_e} &\approx r \cdot m_e + q_1 \cdot (m_{\nu_\mu} + m_{\nu_\tau}) \approx 2r \cdot m_e. \end{aligned} \tag{16}$$

In conclusion, if there is some amount of $W_L - W_R$ mixing, all neutrinos become massive (Dirac) particles. Charged and neutral leptons exhibit similar mass hierarchies.

4 Phenomenology

This section briefly discusses some phenomenological consequences of the present model of electroweak interactions and draws comparisons with existing data or shows which type of experiment may serve to test the theory.

Most gauge models that were proposed for the unification of the known non-gravitational interactions or for an explanation of the generation structure of leptons and quarks are faced with rather stringent lower bounds for the proton lifetime and upper bounds for the branching ratios of lepton-generation number violating processes, most notably for $\mu \to e\gamma$ and $\mu \to 3e$ [19] or $K^0 \to \mu^\pm e^\mp$. If any of those models does not strictly forbid these processes, the gauge bosons responsible for that transition must have masses $\geq 10^{15}\,\mathrm{GeV}$ in the case of proton decay or $\geq 10^5\,\mathrm{GeV}$ for lepton-generation number violating processes [12]. The hierarchy problem becomes then quite prominent. Also, the predictive power of such models is often severely limited by the arbitrariness in the choice of the Higgs sector.

In contrast, TPT strictly conserves baryon number and lepton-generation numbers for topological reasons. Thus positive detection of any of the above-mentioned decays or of neutrino oscillations or double-β decay would necessitate drastic changes in a large part of the topological foundations of TPT and in the theoretical structure based on them. However, contrary to the conventional picture, TPT views quarks and leptons as very different objects; conservation of lepton generations does not imply conservation of quark generations nor preclude quark mixing. (These issues are currently under study, and the potential of H bosons for breaking these hadronic symmetries was noticed in [I].)

On the other hand, TPT positively predicts new particles at the TeV scale. The most spectacular signature arises from hexons because their number by far

exceeds the number of all non-hexon states and because hexons interact strongly, particularly with baryons. Copious hexon production is not expected at Tevatron energies but should take place at the SSC unless hexon masses are substantially higher than presently estimated [6].

According to the extrapolation of QCD to SSC energies [20], the λ lepton is marginally detectable at a collider facility with $\sqrt{s} = 20\,\mathrm{TeV}$ and integrated luminosity $10^{39}\,\mathrm{cm}^{-2}$ if its mass is indeed about 400 GeV. An accelerator with higher energy would be able to cover the whole mass range (deduced in Sect.3.3) in which λ may locate according to the present theory. An interesting open question is whether the direct lepton–hadron couplings postulated by TPT would substantially enhance the production rate for λ and thus allow a more detailed study of its properties. Unfortunately, λ is probably outside the reach of LEP II.

As seen in the previous section, considerable uncertainty persists at this point about the mass predictions for the additional four vector bosons, but at a collider capable of discovering the λ they should be produced in numbers sufficient for their detection. Again according to Ref.[20], a collider with $\sqrt{s} \geq 20\,\mathrm{TeV}$ and $\int \mathcal{L}dt \geq 10^{39}\,\mathrm{cm}^{-2}$ will cover the expected mass range. It may, however, be very hard to distinguish between electroweak vector bosons and hexons if their masses are close and substantial mixing takes place.

H bosons are beyond the reach of e^+e^- colliders. They can be discovered at SSC only if they have appreciable couplings to quarks in baryons – a question whose answer depends crucially on the as yet unknown details of hadron–H couplings. Another potentially important point is that H bosons must be produced in pairs because of lepton-generation number conservation.

Among the indirect detection methods for the predicted particles the one of most immediate interest is a precise measurement of the width of Z^0 because the

existence of a fourth-generation neutrino should reveal itself therein. It may be noted incidentally that the specific superposition corresponding to Z^0 [16]

$$Z^0 = \sqrt{\tfrac{1}{6}}(2V_L^{n\bar{n}} - V_L^{c\bar{c}} + V_R^{c\bar{c}}) \tag{17}$$

has only left-handed couplings to neutrinos, so the counting of neutrino species is the same for this purpose as in the standard model with Weyl neutrinos.

The existence of W_R, $Z^{0\prime}$, $Z^{0\prime\prime}$ and of H bosons at or near the TeV energy range is perfectly compatible with existing experimental data on leptonic weak interactions [21]. The most stringent lower bounds on the mass of W_R in the context of left-right symmetric extensions of the GSW model derive from the analysis of CP violation in the $K^0 - \overline{K}^0$ system [22], but that calculation cannot readily be applied to TPT because neither the mechanism of CP violation nor the precise rules for W_R couplings to quarks in mesons are presently known.

The excellent agreement between the measured anomalous magnetic moment of e or μ [23] with the expectation from QED, augmented by the contribution from presently known hadrons [24], leaves very little room for new particles. An elementary one-loop calculation of the effect Δa of H's on $a \equiv (g-2)/2$ gives (see Fig.11)

$$\Delta a_e \approx \frac{\alpha_f}{4\pi} \cdot \frac{m_e \cdot m_\tau}{M_H^2} \cdot \left(3 - 2\ln\left(M_H^2/m_\tau^2\right)\right) , \tag{18}$$

Both intermediate electrons and λ's may be relevant to the muon anomaly, depending on the masses of H and λ:

$$\Delta a_\mu \approx \frac{\alpha_f}{4\pi} \cdot \left(\frac{m_\mu}{M_H}\right)^2 \cdot \left[\frac{m_\lambda}{m_\mu}\left(3 - 2\ln\frac{M_H^2}{m_\lambda^2}\right) + 4\left(5/3 - \ln\frac{M_H^2}{m_e^2}\right)\right] \tag{19}$$

Assuming that the breaking of parity symmetry does not drastically increase the

couplings of right-handed bosons to leptons, it follows from Ref.[16] that

$$\begin{aligned} \alpha_R &= \frac{g_R^2}{4\pi} \approx \tfrac{1}{2}\alpha_{em.}, \\ \alpha' &= \frac{g_{Z^{0\prime}}^2}{4\pi} \approx \tfrac{2}{3}\alpha_{em.} \end{aligned} \tag{20}$$

and that $Z^{0\prime\prime}$ does not couple to charged leptons. Heavy vector bosons contribute far less to a_e and a_μ than H bosons because the leptons inside the loop are of the same generation as the external ones. Thus, if H's and the new vector bosons have TeV masses and if the Yukawa coupling f takes the value inferred from the mass calculations in Sect.3.3, there is no conflict with experiment.

Potentially much larger are the anomalous magnetic moments produced by the huge numbers of heavy hadrons with which electroweak particles interact. In the context of models of light fermions with a compositeness scale $\Lambda \gg m_f$ it was found both with a dispersion-relation approach [25] and in a parton-model framework [26] that anomalous magnetic moments from the substructure are suppressed at least by a factor m_f/Λ. In the case where the light composite fermion consists of an intermediate-mass fermion F with mass $m_F \ll \Lambda$ and a heavy boson B with $m_B \approx \Lambda$, the suppression was shown to be of order $m_f m_F/m_B^2$. Naive application of these results to the present case sets $m_F \approx m_f = m_l$ where $l = e, \mu$, and $m_B \approx m_0 \geq 1\,\mathrm{TeV}$, so obtaining $a_e^{(hadron)} \lesssim 2.5 \cdot 10^{-13}$ and $a_\mu^{(hadron)} \lesssim 10^{-8}$.

One may see the mechanism producing similar suppression in the present model by studying the discontinuity of the photon–lepton vertex, see Fig.12. Only the J=1 partial wave A_1 enters, from which the term relevant to the magnetic moment has to be extracted. Due to the unitarity bound on partial-wave amplitudes and the fact that the magnetic-moment term in A_1 falls faster than the full A_1 by a factor $s^{-1/2}$, an unsubtracted dispersion relation holds for the anomalous magnetic moment unless the discontinuity fails to vanish at $s = 0$, which is not the case here.

In addition, the softness properties of TPT vertex functions (see Sect.2) imply that $\mathrm{Im}\, A_1$ decreases rapidly for $s > m_0^2$. With the exception of the first term in the second bracket in Fig.12 (to be considered below), $\mathrm{Im}\, A_1 = 0$ for $s < m_0^2$. Hence the discontinuity from intermediate states with hadrons is appreciable only in a small interval above m_0^2, and the dispersion integral for the magnetic moment yields a suppression factor $\sim m_0^{-(1+\epsilon)}$, $\epsilon > 0$, if $\mathrm{Im}\, A_1$ decreases as $s^{-\epsilon/2}$.

The two-lepton intermediate state (first term in the second bracket of Fig.12) contributes over a wider range beginning at $4m_l^2$, but at $s \leq m_0^2$ and the corresponding low t values, the amplitude for lepton–lepton elastic scattering (the bubble below the unitarity cut) is presumably well approximated by the one-hadron exchange diagrams, whereas the vertex softness comes into effect at higher t. The situation is thus quite analogous to the vector-boson exchange terms in Fig.11, and Δa_l is of the order of $(m_l/m_0)^2$, again within the experimental bounds. It is crucial in this context that the PRV's do not contain any low-mass hadron poles or branch cuts, which might in principle emerge from the infinite summation over hadronic corrections implied in the PRV's. This point can be settled only when the elementary hadron–lepton vertices and certain features of the strong-interaction dynamics are understood, but the topological proposals in Appendix A of [I] are likely to have this property. The preliminary conclusion is that no conflict need exist between TPT and present-day magnetic-moment measurements, but that the extra contributions nearly exhaust the experimental margins.

Very critical tests of TPT result from its neutrino sector. It was mentioned above that the existence of a fourth neutrino will have to reveal itself soon in the width of Z^0. The neutrino masses were seen to follow a hierarchy pattern similar to that of charged leptons. The mixing between W_L and W_R, which is responsible for nonvanishing neutrino masses, is in principle a calculable quantity in TPT (see

below). The present upper limit from experiment, $m_{\nu_e} \leq 50\,\mathrm{eV}$ [21], already restricts the mixing angle considerably:

$$\theta_\chi \leq 10^{-3}. \tag{21}$$

If the result $m_\nu \approx 20\,\mathrm{eV}$ of one series of experiments [27] is confirmed, TPT would have to interpret that neutrino as ν_e and hence would require additional neutrino generations around 400 eV, 35 keV and 8 MeV. If also the standard cosmological model and the calculations and measurements of the ^{4}He abundance [28] are trusted (for considerations potentially challenging the conventional picture see, however, [29]), the TPT model is flatly ruled out: TPT neutrinos are absolutely stable; their presence would have increased the expansion rate of the universe and caused an earlier freeze-out of neutrons, leading to a higher ^{4}He abundance than observed. Conversely, if the constraint on neutrino masses following from the cosmological model,

$$\sum_{i=1}^{4} m_{\nu_i} < 100\,\mathrm{eV}, \tag{22}$$

is to be satisfied by TPT, then

$$\begin{aligned} m_{\nu_e} &< 2.5 \cdot 10^{-4}\mathrm{eV}, \\ \theta_\chi &< 5 \cdot 10^{-9}. \end{aligned} \tag{23}$$

The smallness of these numbers justifies a few speculative thoughts about the origin and amount of $W_L - W_R$ mixing in TPT. The graph in Fig.1(a) was recognized to produce such mixing. As it superficially diverges quadratically, a naive estimate using a cut-off m_0 is not very trustworthy, but may nevertheless indicate the order of magnitude of the effect. One expects roughly

$$M_{LR}^2 \approx (e^2/2) f^2 \frac{4\pi^4}{(2\pi)^8} m_0^2 \approx 10^{-7} m_0^2 \tag{24}$$

for $\alpha_f \approx 10^{-3}$. If one assumes that the strong interactions do not produce mixing,

one obtains the mass matrix

$$\mathcal{M}[\mathrm{TeV}^2] \approx \begin{pmatrix} 10^{-2} & 4\cdot 10^{-7} \\ 4\cdot 10^{-7} & 1 \end{pmatrix} \tag{25}$$

for $M_R \approx 1\,\mathrm{TeV}$ and $m_0 \approx 2\,\mathrm{TeV}$, and the mixing angle is

$$\theta_\chi^{(elw.)} \approx \frac{M_{LR}^2}{M_R^2 - M_L^2} \approx 4\cdot 10^{-7}. \tag{26}$$

This estimate is thus two orders of magnitude above the bound (23) imposed on θ_χ by the standard cosmological model.

It is to be expected that strong interactions not only produce M_L and M_R but also mix the two states. The corresponding angle $\theta_\chi^{(str.)}$ cannot be reliably estimated before the precise mechanism for $L-R$ symmetry breaking is known. Generally one may suppose that the mass difference arises because W_L cannot couple to a class of hadron bubbles from which W_R acquires $\Delta m^2 = c^2$, and *vice versa*. The resulting mass matrix

$$\mathcal{M} = \begin{pmatrix} a^2+b^2 & b^2 \\ b^2 & c^2+b^2 \end{pmatrix} \tag{27}$$

yields the masses and the mixing angle

$$\begin{aligned} M_L^2 &\approx a^2 + b^2 \\ M_R^2 &\approx c^2 + b^2 \\ \theta_\chi^{str.} &\approx \frac{b^2}{c^2 - a^2} \approx \frac{b^2}{c^2} \end{aligned} \tag{28}$$

if $b^2 \ll a^2 \ll c^2$. Compliance with the bound (21) restricts the mixing element b^2 to the GeV range unless M_R is substantially heavier than 1 TeV. The future will have to tell whether the necessary mechanism is present in TPT or not.

5 Summary and Outlook

The main purpose of the work presented in [I] and here was to probe the concepts that were developed in the framework of a bootstrap approach to the strong interactions for their applicability in the context of electroweak interactions. Since the topological expansion relates the strength of an interaction to the topological complexity of the two-dimensional surfaces accompanying the relevant Feynman graphs, it was to be expected that unique determination of the new structures would require the synthesis of a great many consistency constraints arising in seemingly disparate areas of TPT.

Clearly, this goal has not been accomplished yet. However, the ease with which TPT accommodates the quantum numbers of all presently known nonhadrons and supplements them with just a few more states of rather plausible characteristics (right-handed vector bosons, a fourth lepton generation and a set of particles connected with the generation structure of leptons) is remarkable. One notes that these predictions mainly flow from the surface *boundary* and are not affected by the specifics of the interactions, which relate to the interior structure of the surface embedding the Feynman graph. It is, then, quite conceivable that several different dynamics are compatible with the quantum-number spectrum of electroweak TPT. Conversely, if the theory presented here does not correctly reproduce certain experimental data, the quantum-number predictions may still be valid but some basic dynamical concepts would have to be abandoned. The very existence of ν_λ, as deducible from the width of Z^0, and the absence of neutrino mixing, double-β decay and other forbidden processes may be regarded as tests of this part of the theory.

The topological basis of the dynamics, namely the surfaces housing Feynman

vertices, was developed in [I] on the assumption that those surfaces contain essentially the same characteristic elements as zero-entropy topologies plus some intrinsic complexity (elementary handles, most notably); the latter was found to be intimately connected to the assumed masslessness of elementary nonhadrons. These features were felt to be most naturally incorporated in a model with a small number of hard, noncontractible vertices as in Lagrangian field theory. The GSW model served as a guide, mainly in the treatment of vector-boson self-interactions; the resulting elementary vertices give rise to Feynman rules which may also be derived from a Lagrangian with only dimensionless coupling constants. The consistency constraints from topology select a specific model and eliminate a substantial part of the arbitrariness inherent in field theory (however, the value of coupling constants is not restricted by the topological structures).

Besides its generally promising phenomenological content (with the neutrino masses looming as a potentially serious difficulty), this Lagrangian model of electroweak TPT also has two major, superficially unrelated, problems: Firstly, several ambiguities in the details of elementary vertex topologies persist, but they do *not* affect the Feynman rules. Either important topological constraints have not been recognized, or there is a puzzling mismatch between the richness of complicated surfaces and the relatively simple elementary vertex functions. The dilemma is even more pronounced in semihadronic interactions. Secondly, the Lagrangian is not renormalizable because some terms do not respect the chiral isospin symmetry connected with the vector bosons. The analysis of several ways to deal with this situation suggests that the assumption of structureless elementary nonhadrons has to be given up in favour of a dynamics which describes them as bound states either of hadrons or of themselves (with or without intervention from hadrons), the compositeness scale being around or above 1 TeV.

An optimistic view of the encountered dilemma interprets the phenomenological successes of the Lagrangian model as an indication that it is a reasonable low-energy approximation of the more complete theory to be developed. The above-mentioned ambiguities in the vertex topologies are seen as originating in their wrongly assumed elementarity. As Appendix B indicates, the door may then also be open for a closer relation between electroweak and strong interactions and a dynamical calculation of the fine-structure constant.

A Finiteness of the Hadronic Topological Expansion

As discussed in Sect.2.1, TPT is not able to absorb infinities that might arise in higher orders of the strong-interaction topological expansion through infinite renormalization of bare parameters. It is therefore crucial that every term in the expansion be finite.

An eventual proof of this important property will rest on the solution of the zero-entropy bootstrap. Meanwhile, the qualitative features of zero-entropy vertex functions and a comparison of the discontinuity structure of higher-order terms with that of zero entropy make it plausible. The zero-entropy equations reduce [1,30] to an infinite set of coupled equations for one single scalar particle by factorization of the contributions of spin, chirality and all internal degrees of freedom. On the mass shell, where all graphs are to be understood in the sense of Landau and Cutkosky rather than as Feynman diagrams, they take the form shown in Fig.13. (Small full dots represent zero-entropy vertex functions; the dashed lines indicate the channel whose associated discontinuity is considered.) These equations arise from unitarity and the so-called *contraction principle* [1] which expresses the duality properties of zero-entropy vertex functions (see also Fig.15(b)). The nonlinearity of the bootstrap problem is manifest in Fig.13: The discontinuity of the vertex functions can be represented by the sum of products of *two* vertex functions. It is this nonlinearity which allows hope for a unique determination of all elementary on-shell amplitudes.

Once the on-shell problem is solved, extension off shell is accomplished by solving an infinite system of coupled *linear* equations, as shown in Fig.14 (heavy lines are off shell): On the right-hand side of the equations for cubic and higher vertices with just one leg off shell, products of one (unknown) off-shell function and one (input)

on-shell vertex appear. The first line of the figure shows this with the example of the three-point function with one leg off shell (which is a constant on the mass shell for kinematical reasons). Once these equations are solved, more and more legs may successively be continued off the mass shell, as the second line of the figure exemplifies through the zero-entropy two-point function (also called trivial vertex). Chew and Levinson investigated some of its properties in connection with higher-order corrections and Feynman rules [9].

A key ingredient in the dynamical scheme of Figs.13 and 14 is the requirement that elementary vertex functions (with the exception of trivial vertices and on-shell cubic vertices) satisfy *unsubtracted* dispersion relations [3]. Without such a property, amplitudes would not be completely determined by their discontinuities and the bootstrap cycle would not properly close. The dispersion approach to quantum field theory shows that the need for subtractions is intimately connected with infinite renormalizations of structureless, hard vertices and pointlike particles. Conversely, one may expect that a theory in which every "elementary" particle is a bound state of all other "elementary" particles remains finite even when radiative corrections are calculated.

The convergence of unsubtracted dispersion relations is closely associated with Regge asymptotic behaviour [31]. It is instructive to compare TPT to the string models [32] which prominently feature Regge trajectories and nevertheless diverge at the one-loop level unless extra symmetries produce cancellations. Their trajectories are linear due to the narrow-resonance approximation [33]; the finite widths of excited states (and unitarity) are restored by loop diagrams, which cannot be transformed away by duality because they correspond to cylindrical and higher surfaces (see Fig.15(a)). It is thus not surprising that loops generally are divergent.

TPT is based on a refined version of the topological expansion present in the

string models and allows the same duality transformations (homotopic deformations of the world sheet in the string picture). A subtle difference in the prescriptions for joining diagrams enables TPT to also contract certain planar loops and thus to incorporate multi-particle singularities in zero-entropy vertex functions as shown in Fig.15(b). (It may be noted that such loop contraction would not be possible if the surfaces of TPT were to have the meaning of a string's world sheet and to carry a Lagrangian density.) The importance of multi-particle intermediate states in the bootstrap mechanism is clearly illustrated by an adaptation [8] to TPT of the ABFST model [34] which formulates the Bethe–Salpeter equation in terms of discontinuities. The infinite series of ladder diagrams produces a bound state (Fig.16) whose mass and residue (in the crossed channel) are required by the bootstrap to match the input mass and coupling. A less drastic approximation [7] replaces the sides of the ladder by reggeons, thus taking into account indefinite numbers of intermediate particles in the s-channel, and finds a coupling constant g which is substantially smaller than the result in [8].

The topological expansion of TPT forbids contraction of nonplanar Feynman loops whose accompanying quark lines undergo switching (for a very brief survey of basic TPT notions see [I], Sect.2). Do noncontractible loops diverge and need subtractions? Figure 14 suggests that zero-entropy vertex functions are so "soft" that the Feynman integral converges and that an unsubtracted dispersion relation gives the real part of the radiative correction in terms of its imaginary part. The latter is seen to have essentially the same structure as the corresponding zero-entropy discontinuity, zero-entropy vertices appearing on either side of the cut. If only colour switches are present, Fig.17 differs from the matching zero-entropy discontinuity Fig.13 only by its action in colour space but not in its analytic structure. The argument is somewhat more involved in the presence of chiral switches, see below.

it will be assumed now that nonplanar loops are equally free of divergences, as no indication to the contrary has been encountered.

Chiral switches produce extra powers of momentum [9], and there is no limit to their number even along a single intermediate line. It is not presently known whether elementary vertex functions are soft enough to absorb the extra momentum factors from any *finite* number of chiral switches – they would have to fall off faster than any power in each of their variables. According to the analysis by Chew and Levinson [9], the situation changes completely, however, when one sums *first* over all degrees of second-kind entropy before one evaluates the loop. It was found that a trivial vertex $M_2^0(p^2)$ (see second line of Fig.14) intervenes between adjacent instances of switching. Denoting the switch operator by $\chi(p)$ (χ is nonsingular) one obtains the series

$$\begin{aligned} iD_\chi(p) &= \frac{i\chi(p)}{p^2-m_0^2} + \frac{i\chi(p)}{p^2-m_0^2}\, iM_2^0(p^2)\frac{i\chi(p)}{p^2-m_0^2} + \dots \\ &= \frac{i\chi(p)}{p^2-m_0^2}\left(1 + M_2^0(p^2)\frac{\chi(p)}{p^2-m_0^2}\right)^{-1} \\ &= i\chi(p)\left(p^2 - m_0^2 + \chi(p)M_2^0(p^2)\right)^{-1}. \end{aligned} \tag{29}$$

As $p^2 \to m_0^2$ (and $p\!\!\!/ \to m_0$), $\chi(p)p\!\!\!//p^2 \to cst.$, and $M_2^0(p^2) \sim (p^2-m_0^2)^2$. One sees that the high-energy behaviour of D_χ becomes independent of $\chi(p)$ if $\chi(p)M_2^0(p^2)$ increases more rapidly than p^2. It has been conjectured [9] that $M_2^0(p^2)$ itself should increase at least as $p^2\ln(p^2/m_0^2)$, and $\chi(p)$ is proportional to p^2 for mesons, p^3 for baryons and p^4 for hexons; so indeed

$$D_\chi(p) \longrightarrow \left(M_2^0(p^2)\right)^{-1}, \quad p^2 \to \infty. \tag{30}$$

Loop diagrams with indefinite numbers of switches are thus no more divergent than the corresponding diagrams without switches.

In summary, the convergence of higher-order terms in the topological expansion is an important open question in TPT for whose final solution deeper understanding

of the general properties of elementary vertex functions will be required. It appears, however, that the absence of structureless elementary particles gives a fundamental meaning to the cut-off associated with the size of a bound state in phenomenological models of composite systems. In other words, the bootstrap dynamics at the basis of the topological expansion incorporates in the elementary vertices infinite numbers of diagrams that would be divergent in the usual field theories. Noncontractible loops seem to behave in essentially the same way as the contractible ones included in the bootstrap and therefore very likely do not pose any new problems.

B A Bootstrap Model for Electroweak Vertex Functions

Section 2 discussed the reasons why TPT appears to require some sort of bootstrap mechanism not only for hadrons but also for electroweak particles: Point-like elementary particles are beset with ultraviolet-divergent radiative corrections which – if they can be absorbed by infinite renormalization of bare parameters – destroy whatever relations there may exist between strong and electroweak coupling constants. A successful bootstrap theory of particles must determine these quantities dynamically.

The model which will be outlined here serves mainly illustrative purposes and does not pretend to be fully consistent and to fulfill all requirements of Sect.2. It takes the electroweak particle spectrum developped in [I] and supposes that the electroweak interactions are induced by the strong interactions in such a way that the "elementary" electroweak vertices show structure associated with hadrons and strong interactions at the scale m_0. No further scales, particles and interactions are thereby introduced. Elementary nonhadrons appear as bound states of hadrons and elementary nonhadrons, manifesting the circularity of their bootstrap origin. It is anticipated that the conservation of electric charge will play a central role in this approach. No attempt is made to interpret the electroweak particles as hadron states whose properties underwent drastic changes as higher and higher orders of the topological expansion were included. The appearance of lepton numbers and their very strict conservation would presumably be hard to understand from such a point of view.

The present scheme is directly inspired by the system of equations in Fig.A.2, which allow extension of zero-entropy vertex functions away from the mass shell.

There, (unsubtracted) dispersion relations determine the real parts of off-shell amplitudes, which are in turn given by the sum of products of off-shell and on-shell vertex functions. One may hope to determine (off-shell) electroweak semihadronic vertices from their *hadronic* discontinuities, expressed as products of semihadronic and hadronic amplitudes. Purely nonhadronic vertices are afterwards obtained through their discontinuities consisting of products of semihadronic vertices. This procedure represents the direct analogy of the method which allows determination of zero-entropy vertices with several legs off the mass shell.

The critical ingredient in the zero-entropy counterpart of the proposed scheme is the idea of *contraction*: Only those connected sums of zero-entropy topologies contribute to the system which again result in a zero-entropy topology. A similar restriction is needed in the electroweak context to achieve a closed set of equations. Above the levels $g_1 = g_3 = g_4 = 0$, $g_2 = 0, 1$, however, no single term in the topological expansion has this self-building capacity. Nevertheless, an infinite class of diagrams, representing the sum over all values of a specific entropy index, may be considered a single object and as such may have that capacity again. For example, one may restrict oneself to planar graphs ($g_1 = g_2 = 0$) without nonhadron loops ($g_5 = 0$) and sum over all values of g_3 and g_4. Any planar plug between any two members of this class which does not produce a nonhadron loop again falls into the same class.

Figure 18 shows the first few terms in a first set of equations in graphical form; vertices with H bosons are analogous and were omitted for simplicity. The case shown corresponds to planar discontinuities only; accordingly, the blobs contain all planar graphs without internal nonhadrons and with indefinite values of g_3 and g_4. The system extends indefinitely and includes graphs with any number of vector bosons, H-boson and lepton pairs on the left side of the cut and any number of

hadrons on the right side. As in the zero-entropy situation, it is assumed (and postulated) that unsubtracted dispersion relations close the circle.

Three features of Fig.18 are particularly worth noting:

1. The discontinuities begin at m_0^2 or $4m_0^2$, far from the experimentally investigated kinematic region. While the low-energy phenomena in this model may closely mimick the predictions of the GSW model, the high-energy effects will be more similar to those in some composite models.

2. The manifest linearity of these equations implies that each semihadronic vertex can only be determined up to a multiplicative constant which is independent of the corresponding factors in other semihadronic vertices.

3. Semihadronic vertices lack the cyclic symmetry of zero-entropy amplitudes. Their full determination requires another set of equations where nonhadrons appear on either side of the cut, in analogy to the calculation of zero-entropy vertex functions with several legs off shell.

The graphical equations of Fig.18 may be summarized in highly condensed notation by a pair of integral operator relations:

$$\begin{aligned} \Delta_h^{pl.}\mathbf{V} &= 2i\,\mathbf{V}\rho_{pl.}\mathbf{M}^\dagger, \\ \mathrm{Re}\,\mathbf{V}(x) &= (2\pi i)^{-1}\int_{-\infty}^{+\infty}\frac{dx'}{x'-x}\Delta_h^{pl.}\mathbf{V}(x'). \end{aligned} \tag{31}$$

$\mathbf{M}$ stands for the totality of planar hadronic vertex functions (including any number of external lines), $\mathbf{V}$ represents the semihadronic vertices; $\Delta_h^{pl.}\mathbf{V}$ is the planar discontinuity of $\mathbf{V}$, restricted to hadron intermediate states. The phase space operator $\rho_{pl.}$ performs all appropriate (planar) phase space integrals for the intermediate states in the discontinuity.

Performing cuts on semihadronic vertices in different ways yields another set of equations, two typical examples of which are shown in Fig.19. The discontinuities in graphs with only hadrons and vector bosons exclusively contain hadrons; intermediate vector bosons contribute to electroweak radiative corrections of semihadronic vertices. The situation is different in the presence of leptons and H bosons where lepton number conservation requires nonhadrons in the intermediate state if semihadronic amplitudes are to be determinable from their discontinuities. Figure 19 corresponds to the equations

$$\begin{aligned} \Delta^{pl.}_{h,l}\mathbf{V} &= 2i\,\mathbf{V}\rho_{pl.}\mathbf{V}^\dagger, \\ \mathrm{Re}\,\mathbf{V}(y) &= (2\pi i)^{-1}\int_{-\infty}^{+\infty}\frac{dy'}{y'-y}\Delta^{pl.}_{h,l}\mathbf{V}(y') \end{aligned} \tag{32}$$

where $\Delta^{pl.}_{h,l}\mathbf{V}$ indicates the discontinuity of semihadronic vertex functions with hadrons and – where necessary – leptons and H bosons in the intermediate state. (32) shows that these new equations are nonlinear. One thus expects that the multiplicative constants which were arbitrary in the equations (31) are determined by these extra conditions. Comparison of Fig.19(a) with the second line of Fig.18 suggests that the two-photon–two-hadron coupling constant is roughly the square of the one-photon coupling. Of course, the issue of current conservation is intimately connected with this property; a more detailed discussion will follow below.

A central question is whether the two sets of equations are mutually compatible. No proof (nor disproof) has been found at this point; a positive indication may be seen in the fact that (31) is linear in $\mathbf{V}$ and features a dispersion relation in a single variable, all others being kept fixed. (32) yields equations for all other (planar) variables and relates the corresponding discontinuities to the full amplitudes again via single-variable dispersion relations. It will thus be assumed below that no inconsistency arises.

The stage is now set for equations relating purely nonhadronic vertex functions (summarized by an operator $\mathbf{W}$) to the semihadronic amplitudes $\mathbf{V}$. Following the basic ideas outlined at the beginning of this Appendix, one constructs $\mathbf{W}$ from its discontinuity in which nonhadrons again occur only to the extent required by lepton-generation number conservation. The corresponding equation thus is

$$\begin{aligned} \Delta^{pl.}_{h,l}\mathbf{W} &= 2i\,\mathbf{V}\rho_{pl.}\mathbf{V}^\dagger, \\ \mathrm{Re}\,\mathbf{W}(z) &= (2\pi i)^{-1}\int_{-\infty}^{+\infty}\frac{dz'}{z'-z}\Delta^{pl.}_{h,l}\mathbf{W}(z'). \end{aligned} \tag{33}$$

It is simpler to solve than (31) and (32) – once $\mathbf{V}$ is known – because $\mathbf{W}$ does not appear on the right-hand side of the first line. Examples from its graphical counterpart are given in Fig.20.

The problem of current conservation – already encountered in connection with $\mathbf{V}$ – is even more pressing for $\mathbf{W}$. It is not at all clear how the fairly complex pattern of Yang–Mills couplings should arise from the described dynamics. Given the algebraic nature of current conservation and gauge symmetry, it is conceivable that the question is amenable to a formal algebraic treatment and can be answered without explicitly solving this particular dynamical system.

The following observation may indicate that a thorough investigation is needed before this or similar bootstrap schemes can be dismissed (or accepted). As mentioned above, Fig.19(a) suggests that the two-photon coupling is weaker than the one-photon coupling – proportional to e^2 rather than e if one is optimistic; similarly, an n-photon vertex would carry a factor e^n. One then expects the cubic Yang–Mills vertex also to be proportional to e^3, its discontinuity structure closely resembling that of a semihadronic vertex with three vector bosons. Closer examination of the peripheral quark lines in the planar bubbles reveals, however, that they are determined by the external hadrons in Fig.19(a) while they are free in Fig.20(a). Accordingly, in the latter equation the weight of each term is higher by

a factor $N \sim 10^2$ (4^2 generations, 2 isospins, 2 spins), which may well compensate the unwanted factor e^2:

$$\alpha N \sim O(1). \tag{34}$$

In a similar way, the quartic Yang–Mills term, Fig.20(d), is of order e^2 rather than e^4.

In conclusion of this outline it needs to be remarked that a scheme of this kind, implying an infinite set of basic electroweak vertices, will put specific constraints on the topological representation of these amplitudes. It remains to be seen whether or not the proposals of [I] are compatible with them. It would suit the bootstrap spirit well if some ambiguities which had remained in [I] would thereby be eliminated.

Acknowledgment

The work described in this paper would not have been possible without the constant criticism and advice of Geoffrey. F. Chew to whom the author is very much indebted. Discussions with Jerry Finkelstein, Henry P. Stapp and Mahiko Suzuki were also very helpful in clarifying many points in this paper. Support was provided by the Director, Office of Energy Research, Office of High-Energy and Nuclear Physics, Division of High-Energy Physics of the U.S. Department of Energy under Contract DE–AC03–76SF00098.

References

[1] G.F. Chew and V. Poénaru, *Z. Phys. C* **11**, 59 (1981).

[2] G.F. Chew and V. Poénaru, *Phys. Rev. D* **32** No.10 (1985).

[3] G.F. Chew, *"Topological Bootstrap Theory of Particles"* (book in preparation).

[4] G. Veneziano, *Nucl. Phys.* **B74**, 365 (1974) and *Phys. Lett.* **52B**, 220 (1974).

[5] G.F. Chew and C. Rosenzweig, *Phys. Rep.* **41C**, 263 (1978).

[6] G.F. Chew, D. Issler, B. Nicolescu and V. Poénaru, in *Proceedings of the Hadronic Session of the XIX^e Rencontre de Moriond*, edited by J. Tran Thanh Van (Edition Frontières, Gif-sur-Yvette, 1984), p.143.

[7] L.A.P. Balázs, P. Gauron and B. Nicolescu, *Phys. Rev. D* **29**, 533 (1984).

[8] R. Espinosa, *Nuovo Cim.* **88A**, 185 (1985).

[9] G.F. Chew and M. Levinson, *Z. Phys. C* **20**, 19 (1983).

[10] D. Issler, Lawrence Berkeley Laboratory preprint LBL–19045 (October 1985).

[11] G.F. Chew and D. Issler, *Phys. Rev. Lett.* **55**, 473 (1985).

[12] R.N. Cahn and H. Harari, *Nucl. Phys.* **B176**, 135 (1980).

[13] G. 't Hooft, *Nucl. Phys.* **B72**, 461 (1974).

[14] G.F. Chew, *Phys. Rev. Lett.* **47**, 764 (1981).

[15] J.D. Bjorken and S.D. Drell, *"Relativistic Quantum Fields"*, ch.19 (McGraw-Hill, New York 1965).

[16] G.F. Chew and J. Finkelstein, *Phys. Rev. Lett.* **50**, 795 (1983).

[17] G.F. Chew, private communication (Berkeley, 1985).

[18] G.F. Chew, *Phys. Rev. D* **27**, 976 (1983).

[19] W. Bertl *et al.*, *Phys. Lett.* **140B**, 299 (1984) and *Nucl. Phys.* **B260**, 1 (1985).

[20] E. Eichten, I. Hinchliffe, K. Lane and C. Quigg, *Rev. Mod. Phys.* **56**, 579 (1984).

[21] Particle Data Group, Review of Particle Properties, *Rev. Mod. Phys.* **56**, S1 (1984).

[22] M. Bander, G. Beall and A. Soni, *Phys. Rev. Lett.* **48**, 848 (1982).

[23] P.B. Schwinberg, R.S. van Dyck and H.G. Dehmelt, *Phys. Rev. Lett.* **47**, 1679 (1981).

[24] T. Kinoshita and W.B. Lindqvist, *Phys. Rev. Lett.* **47**, 1573 (1981); T. Kinoshita, B. Nižić and Y. Okamoto, *Phys. Rev. Lett.* **52**, 717 (1984).

[25] G.L. Shaw, D. Silverman and R. Slansky, *Phys. Lett.* **94B**, 57 (1980).

[26] S.J. Brodsky and S.D. Drell, *Phys. Rev. D* **22**, 2236 (1980).

[27] S. Boris *et al.*, *Phys. Lett.* **159B**, 217 (1985).

[28] A.D. Dolgov and Ya.B. Zeldovich, *Rev. Mod Phys.* **53**, 1 (1981), and references therein.

[29] G.R. Burbidge, J.V. Narlikar and A. Hewitt, *Nature* **317**, 413 (1985).

[30] H.P. Stapp, *Phys. Rev. D* **27**, 2445 (1983).

[31] G.F. Chew, *"The Analytic* S *Matrix; a Basis for Nuclear Democracy"*, W.A.Benjamin, Inc., New York 1966, and references therein.

[32] J. Scherk, *Rev. Mod. Phys.* **47**, 123 (1975).

[33] G. Veneziano, *Nuovo Cim.* **57A** 190 (1968) and *Phys. Rep.* **9C** 199 (1974).

[34] D. Amati, S.Fubini and A. Stanghellini, *Nuovo Cim.* **26**, 896 (1962); L. Bertocchi, S. Fubini and M. Tonin, *Nuovo Cim.* **25**, 626 (1962).

Figure Captions

Fig.1: Quadratically divergent graph contributing to $W_L - W_R$ mixing.

Fig.2: Electroweak radiative corrections to lepton propagator.
(a) No further corrections from hadrons.
(b) With hadronic insertions, indicated by shaded blobs.

Fig.3: Example of a skeleton graph. Hadronic self-energy contributions and vertex corrections are represented by shaded circles; dotted boxes show *electroweak* corrections.

Fig.4: Discontinuity structures of (a) vector-boson self-energy and (b) cubic Yang–Mills vertex. Thick lines represent (heavy) hadrons.

Fig.5: Examples of vertices with leptons and/or H bosons.

Fig.6: Mass-generating self-energy insertions for (a) H bosons and (b) vector bosons.

Fig.7: Lepton mass terms resulting from chiral-symmetry-breaking lepton–hadron couplings. (The vacuon Θ is represented by open-circled lines).

Fig.8: Leading contributions to light charged-lepton masses.

Fig.9: A hadronic correction to Fig.8(a).

Fig.10: Neutrino masses induced by $W_L - W_R$ mixing.

Fig.11: Non-standard electroweak contributions to the anomalous magnetic moments of charged leptons.

Fig.12: Discontinuity of the partially renormalized lepton–photon vertex.

Fig.13: The on-shell zero-entropy bootstrap equations.

Fig.14: Off-shell extension of zero-entropy vertex functions. Analogous equations result for all elementary vertices with any number of legs off shell on both sides of the Landau–Cutkosky cut.

Fig.15: Illustration of the difference between string-model and TPT contraction rules. (a) String models retain closed boundary components like A. The surface resulting from the plug is a cylinder which may be homotopically deformed. (b) In TPT, quark lines consist of two halves ($[\alpha,\beta]$ or $[\alpha',\beta']$); in zero-entropy plugs one must erase matching halves ($\alpha-\alpha',\beta-\beta'$) and so again arrives at a disk. Subsequently, the empty Feynman loop contracts to a point.

Fig.16: ABFST ladder model as an approximation to the full bootstrap equations.

Fig.17: Discontinuity of a loop diagram of non-zero entropy. The crosses denote chiral and/or colour switches.

Fig.18: First set of discontinuity equations for semihadronic vertex functions. The system continues indefinitely, including vertices with any numbers of vector bosons and lepton or H-boson pairs.

Fig.19: Examples from second set of discontinuity equations for semihadronic vertex functions. Note the nonlinearity of the system. In (b), a lepton occurs in the intermediate state; there is, however, no term without intermediate hadrons.

Fig.20: Some examples of discontinuity equations for nonhadronic vertex functions.

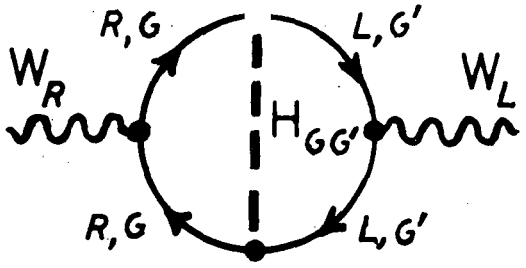

Fig. 1

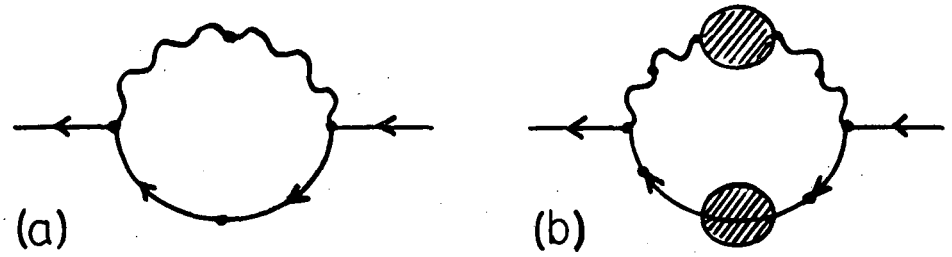

Fig. 2

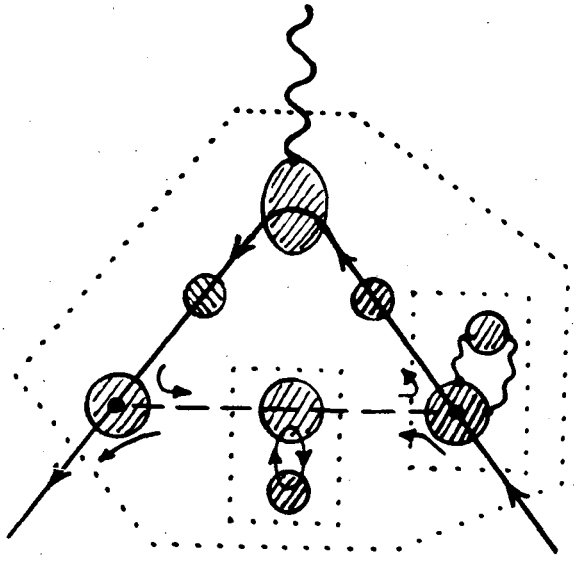

Fig. 3

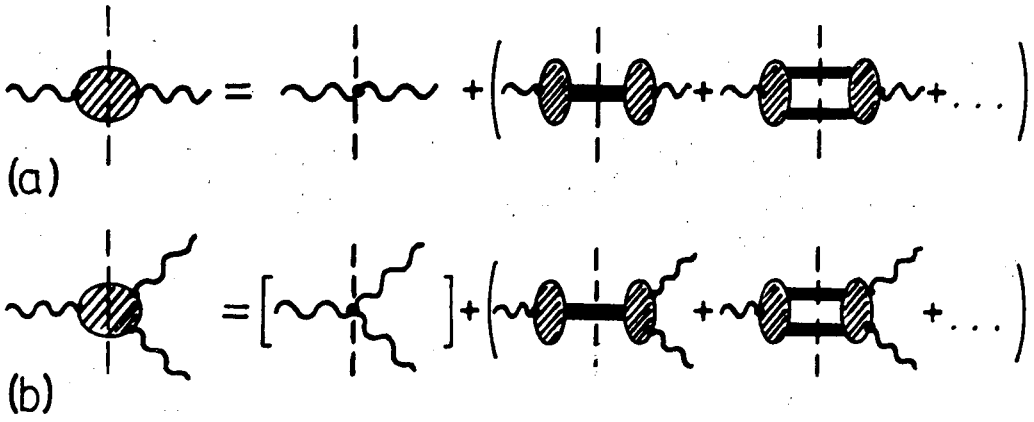

Fig. 4

Fig. 5

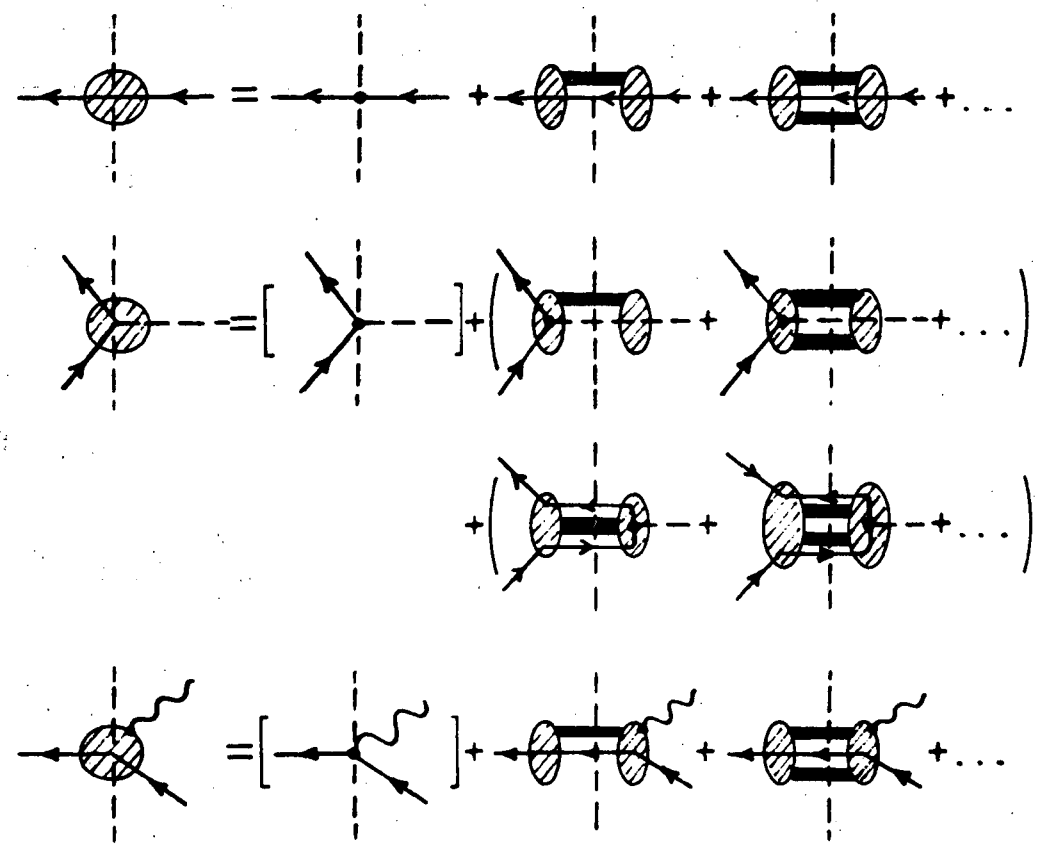

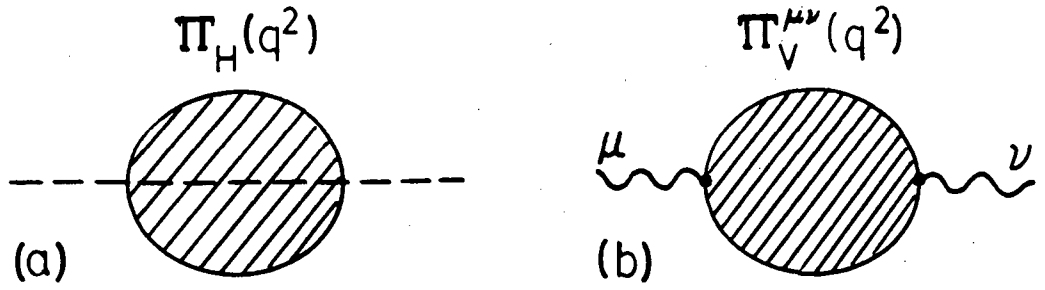

Fig. 6

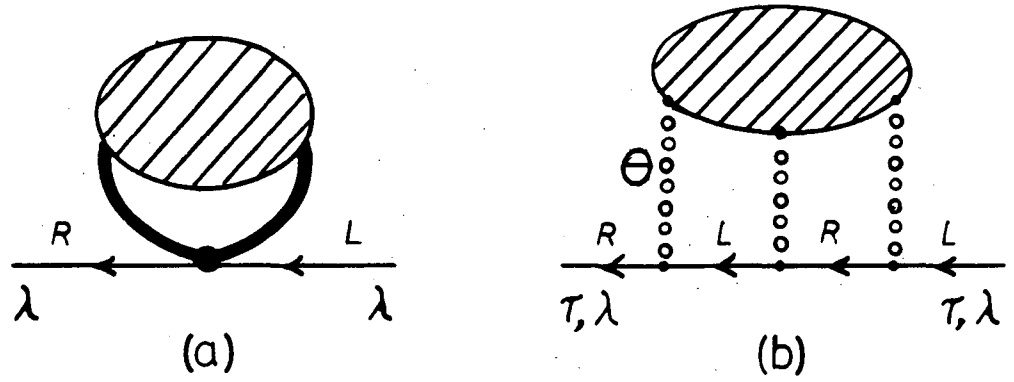

Fig. 7

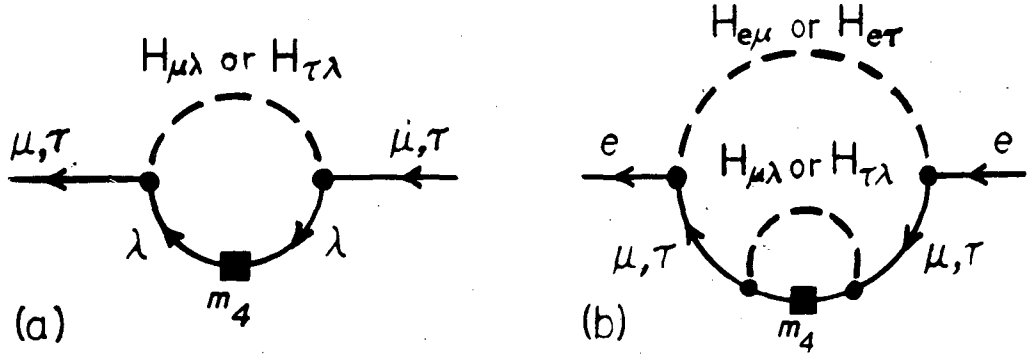

Fig. 8

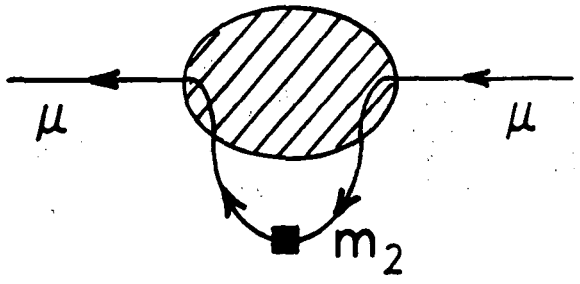

Fig. 9

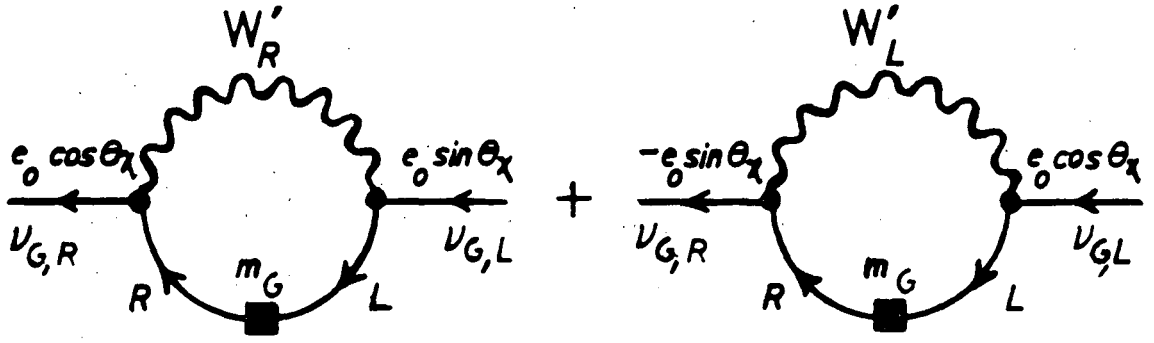

Fig. 10

Fig. 11

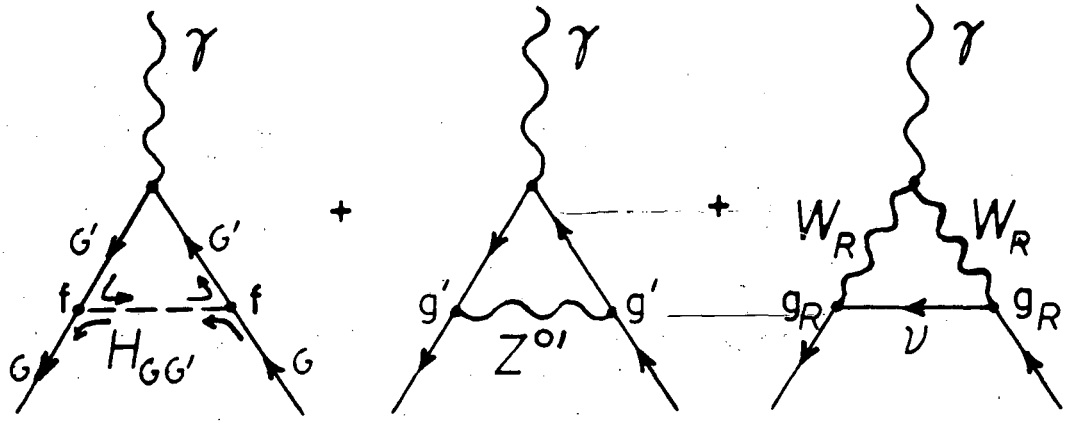

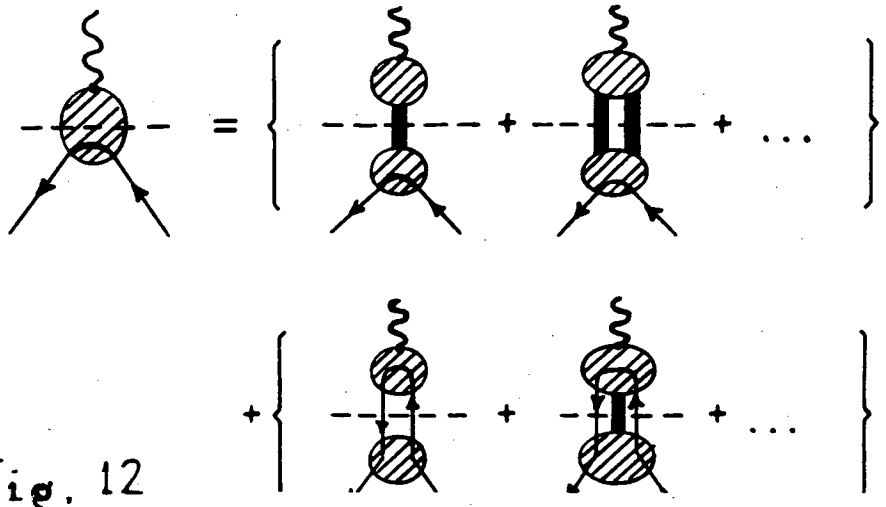

Fig. 12

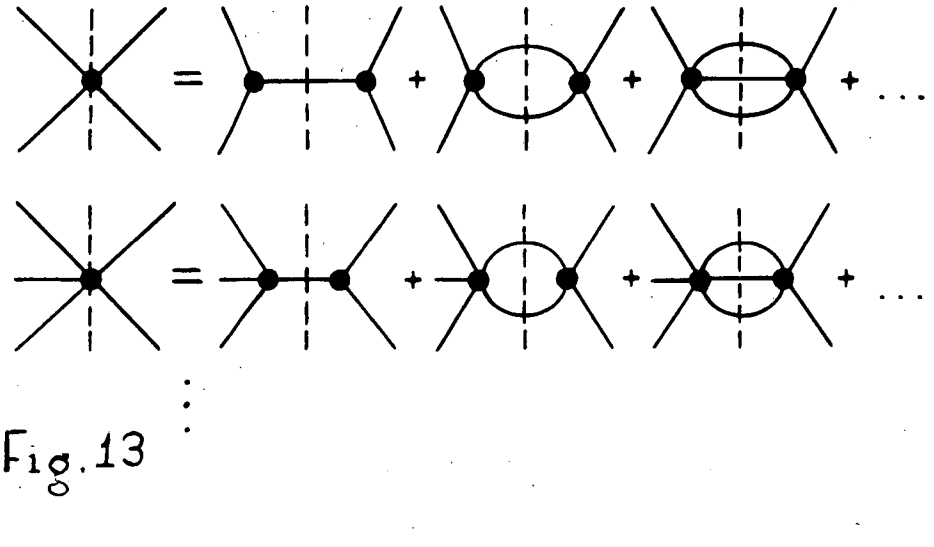

Fig. 13

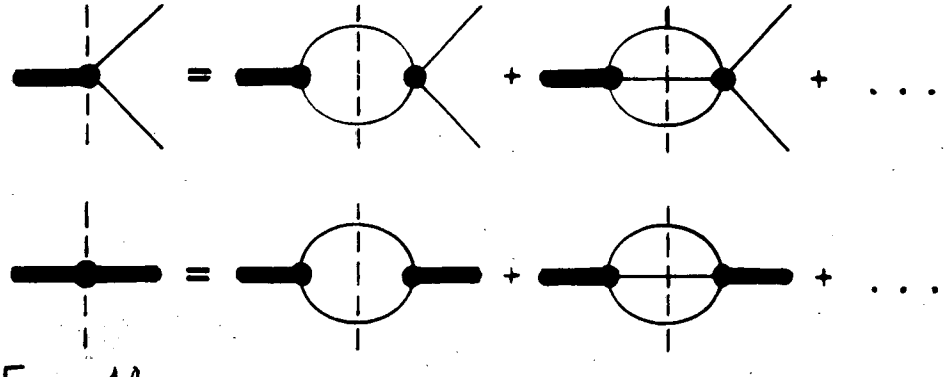

Fig. 14

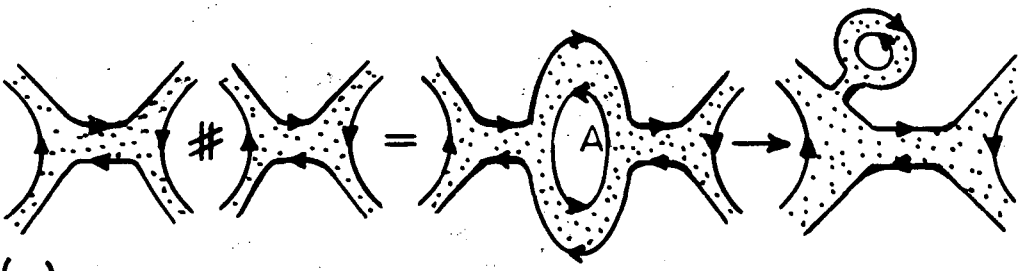

(a)

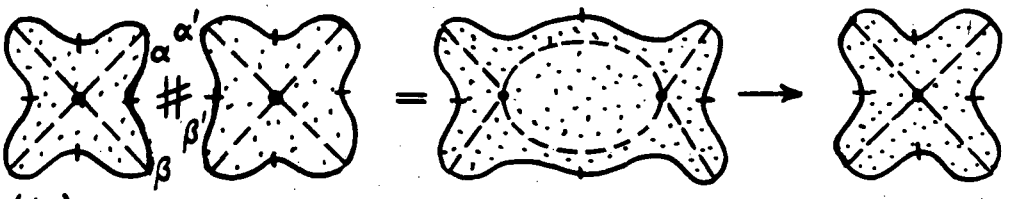

(b)

Fig. 15

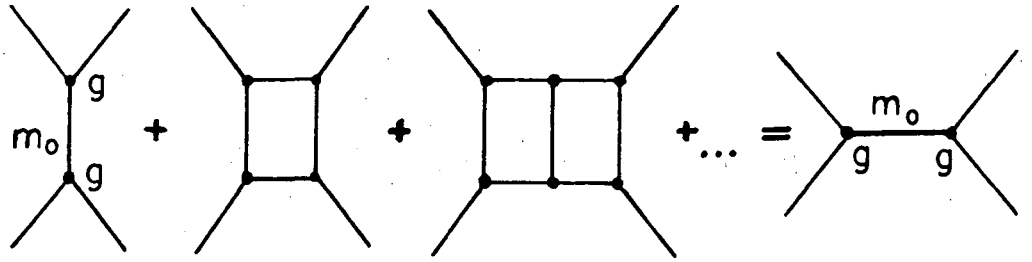

Fig. 16

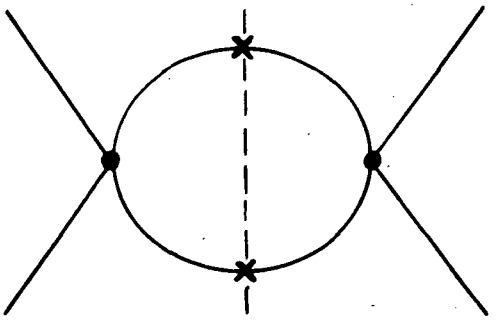

Fig. 17

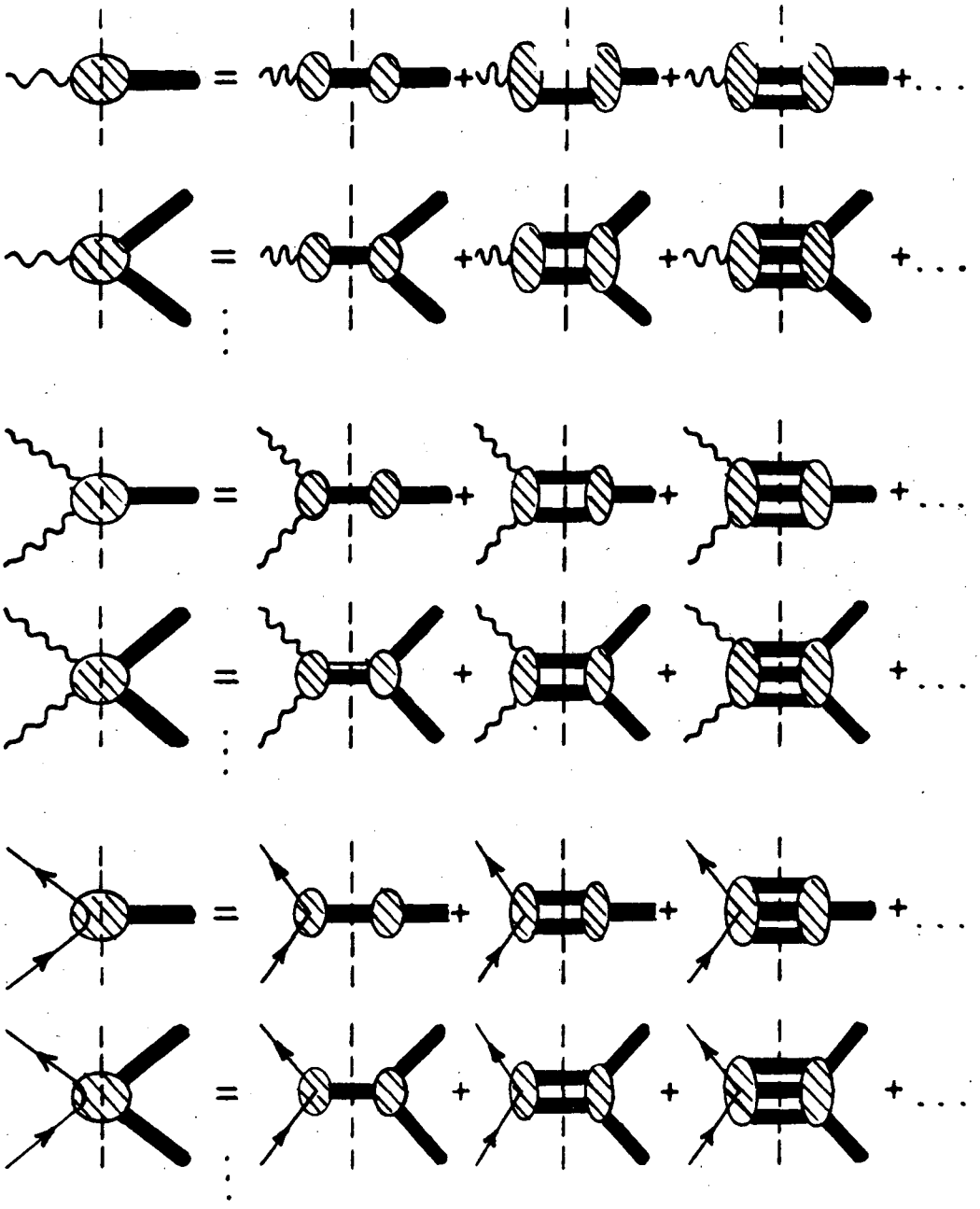

Fig. 18

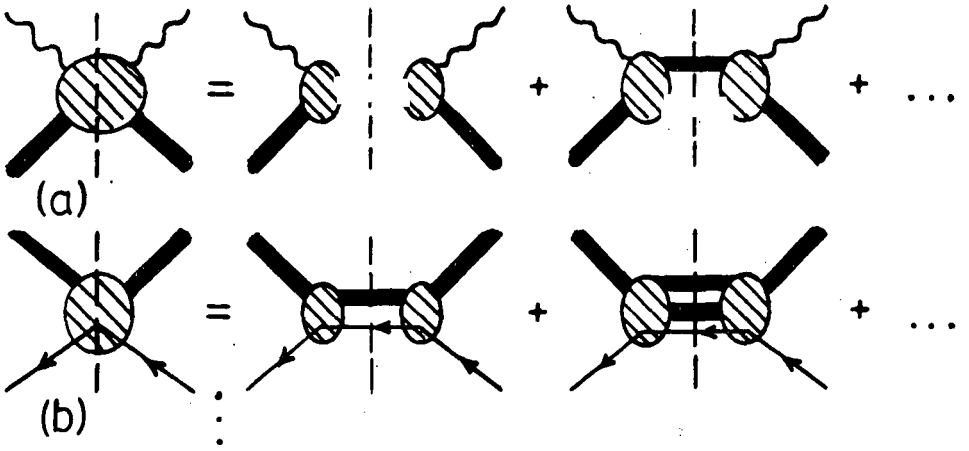

Fig. 19

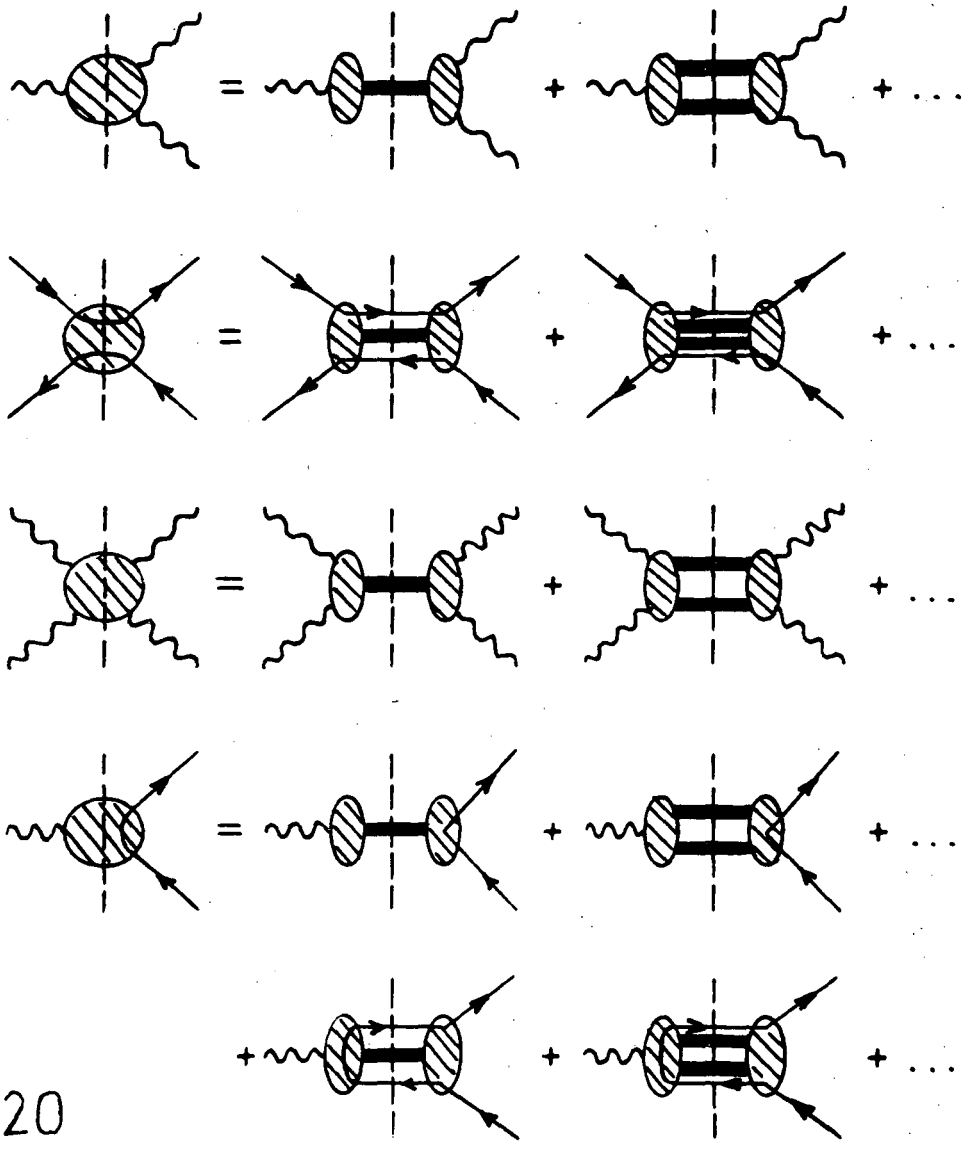

Fig. 20

LAWRENCE BERKELEY LABORATORY
TECHNICAL INFORMATION DEPARTMENT
UNIVERSITY OF CALIFORNIA
BERKELEY, CALIFORNIA 94720